

# Statistical Field Estimation for Complex Coastal Regions and Archipelagos<sup>☆</sup>

Arpit Agarwal<sup>a</sup>, Pierre F. J. Lermusiaux<sup>b</sup>

*Massachusetts Institute of Technology, Cambridge, MA-02139, USA*

<sup>a</sup>*e-mail:* [arpit@mit.edu](mailto:arpit@mit.edu)

<sup>b</sup>*e-mail:* [pierrel@mit.edu](mailto:pierrel@mit.edu)

---

## Abstract

A fundamental requirement in realistic ocean simulations and dynamical studies is the optimal estimation of gridded fields from the spatially irregular and multivariate data sets that are collected by varied platforms. In this work, we derive and utilize new schemes for the mapping and dynamical inference of ocean fields in complex multiply-connected domains and study the computational properties of these schemes. Specifically, we extend a multiscale Objective Analysis (OA) approach to complex coastal regions and archipelagos. Bayesian-based OAs using covariances as inputs commonly require an estimate of the distances between data and model points, without going across complex landforms. New OA schemes based on estimating the length of shortest sea paths using the Level Set Method (LSM) and Fast Marching Method (FMM) are thus derived, implemented and utilized in idealized and realistic ocean cases. An FMM-based methodology for the estimation of total velocity under geostrophic balance in complex domains is also presented. Comparisons with other OA approaches are provided, including those using stochastically forced partial differential equations (SPDEs). We find that the FMM-based OA scheme is the most efficient and accurate. We also show that the FMM-based field maps do not require postprocessing (smoothing). Mathematical and computational properties of our new OA schemes are studied in detail, using fundamental theorems and illustrations. We find that higher-order FMM's schemes improve accuracy and that a multi-order scheme is efficient. We also provide solutions that ensure the use of positive-definite covariances, even in complex

---

<sup>☆</sup>We are grateful to the Office of Naval Research for research support under grants N00014-07-1-1061 and N00014-08-1-1097 (ONR6.1), N00014-07-1-0473 (PhilEx), S05-06 and N00014-08-1-0680 (PLUS) to the Massachusetts Institute of Technology.

## Report Documentation Page

Form Approved  
OMB No. 0704-0188

Public reporting burden for the collection of information is estimated to average 1 hour per response, including the time for reviewing instructions, searching existing data sources, gathering and maintaining the data needed, and completing and reviewing the collection of information. Send comments regarding this burden estimate or any other aspect of this collection of information, including suggestions for reducing this burden, to Washington Headquarters Services, Directorate for Information Operations and Reports, 1215 Jefferson Davis Highway, Suite 1204, Arlington VA 22202-4302. Respondents should be aware that notwithstanding any other provision of law, no person shall be subject to a penalty for failing to comply with a collection of information if it does not display a currently valid OMB control number.

1. REPORT DATE <b>09 APR 2011</b>	2. REPORT TYPE	3. DATES COVERED <b>00-00-2011 to 00-00-2011</b>		
4. TITLE AND SUBTITLE <b>Statistical Field Estimation for Complex Coastal Regions and Archipelagos</b>			5a. CONTRACT NUMBER	
			5b. GRANT NUMBER	
			5c. PROGRAM ELEMENT NUMBER	
6. AUTHOR(S)			5d. PROJECT NUMBER	
			5e. TASK NUMBER	
			5f. WORK UNIT NUMBER	
7. PERFORMING ORGANIZATION NAME(S) AND ADDRESS(ES) <b>Massachusetts Institute of Technology, Cambridge, MA, 02139</b>			8. PERFORMING ORGANIZATION REPORT NUMBER	
9. SPONSORING/MONITORING AGENCY NAME(S) AND ADDRESS(ES)			10. SPONSOR/MONITOR'S ACRONYM(S)	
			11. SPONSOR/MONITOR'S REPORT NUMBER(S)	
12. DISTRIBUTION/AVAILABILITY STATEMENT <b>Approved for public release; distribution unlimited</b>				
13. SUPPLEMENTARY NOTES				
14. ABSTRACT <b>A fundamental requirement in realistic ocean simulations and dynamical studies is the optimal estimation of gridded fields from the spatially irregular and multivariate data sets that are collected by varied platforms. In this work, we derive and utilize new schemes for the mapping and dynamical inference of ocean fields in complex multiply-connected domains and study the computational properties of these schemes. Specifically, we extend a multiscale Objective Analysis (OA) approach to complex coastal regions and archipelagos. Bayesian-based OAs using covariances as inputs commonly require an estimate of the distances between data and model points, without going across complex landforms. New OA schemes based on estimating the length of shortest sea paths using the Level Set Method (LSM) and Fast Marching Method (FMM) are thus derived, implemented and utilized in idealized and realistic ocean cases. An FMM-based methodology for the estimation of total velocity under geostrophic balance in complex domains is also presented. Comparisons with other OA approaches are provided, including those using stochastically forced partial differential equations (SPDEs). We find that the FMM-based OA scheme is the most efficient and accurate. We also show that the FMM-based field maps do not require postprocessing (smoothing). Mathematical and computational properties of our new OA schemes are studied in detail using fundamental theorems and illustrations. We find that higher-order FMM's schemes improve accuracy and that a multi-order scheme is efficient. We also provide solutions that ensure the use of positive-definite covariances, even in complex multiply-connected domains.</b>				
15. SUBJECT TERMS				
16. SECURITY CLASSIFICATION OF:  a. REPORT <b>unclassified</b>			17. LIMITATION OF ABSTRACT  <b>Same as Report (SAR)</b>	18. NUMBER OF PAGES  <b>63</b>
b. ABSTRACT  <b>unclassified</b>			19a. NAME OF RESPONSIBLE PERSON	
c. THIS PAGE  <b>unclassified</b>				



multiply-connected domains.

*Key words:*

Field mapping, Gauss-Markov estimation, Coastal objective analysis, Fast Marching Method, Level Set Method, Geostrophy, Levitus climatology, World Ocean Atlas (WOA), Archipelago.

---

## 1. Introduction and Motivation

Statistical field estimation theory was introduced by Gandin (1965) to the field of meteorology and was extended to oceanography by Bretherton et al. (1976) where it is commonly referred to as Objective Analysis (OA). The theory is based on the Gauss-Markov theorem (Plackett, 1950), and it provides a sound basis for interpolating irregularly spaced data onto a computational grid. Up to specifics of oceanic and atmospheric fields, for example the multiple scales, the OA scheme is equivalent to utilize the update steps of the Kalman Filter to grid the irregularly-spaced data. Specifically, the data is gridded based on specified prior field estimates and error covariance matrices. The OA methodology has been well formulated for open oceans without any landforms (convex simply-connected domains), but the OA in complex coastal regions (multiply-connected domains) is one of the ‘last’ mapping problems which remains to be studied in detail. This is one of the main research questions of the present work.

Our research is completed using the Multidisciplinary Simulation, Estimation and Assimilation System (Haley and Lermusiaux, 2010; MSEAS, 2010). MSEAS consists of a set of mathematical models and computational methods for ocean predictions and dynamical diagnostics, for data assimilation and data-model comparisons, and for optimization and control of autonomous ocean observation systems. It is used for basic and fundamental research and for realistic simulations and predictions, recently including monitoring (Lermusiaux, 2007), real-time acoustic-ocean predictions (Xu et al., 2008; Lermusiaux et al., 2010) and environmental management (Cos-sarini et al., 2009). Several dynamical models are part of MSEAS, including a free-surface primitive-equation dynamical model which uses implicit two-way nesting (Haley and Lermusiaux, 2010). This new multiscale free-surface code builds on the primitive-equation model of the Harvard Ocean Prediction System (HOPS, Haley et al. (2009)). Additionally, barotropic tides are calculated from an inverse tidal model (Logoutov and Lermusiaux, 2008; Lo-

goutov, 2008).

In the multiscale OA schemes of MSEAS, the Kalman updates for data gridding are carried out successively, from the largest scale (uniform mean prior) to the smallest scale, using sequential processing of observations and scale separation. In a two-scale version, a two-staged OA approach (Lermusiaux, 1997, 1999) maps the data onto oceanic fields in two steps: the larger and the smaller scale steps. The main inputs to one of these steps are the statistical description of the field being estimated and the observational noise covariance. While the latter is dependent on the measurement sensor, the knowledge of the field statistics does not come easily in oceanography due to the scarcity of observations. The field statistics is often provided by analytical correlation functions which depend on the spatial separation distance and the spatial-temporal scales (Carter and Robinson, 1987). Other MSEAS schemes also utilize 4D dynamical models to construct covariances (Lermusiaux et al., 2000; Lermusiaux, 2002). These dynamical models are sometimes successfully simplified to diffusion models (Lynch and McGillicuddy, 2001) and this approach is also used here to benchmark our new schemes.

Our work on new OA methodologies for complex coastal regions is motivated by the Philippines Straits Dynamics Experiment (PhilEx, Gordon et al. (2011)). The goal of PhilEx is to enhance understanding of the oceanographic processes and features arising in and around straits, and to improve the capability to predict the inherent spatial and temporal variability of complex Archipelago regions using models and advanced data assimilation techniques. In addition to the Philippines, we have used our new schemes in several coastal regions with and without islands, including the Taiwan region, New England shelf, Dabob Bay and Monterey Bay (Xu et al., 2008; Lermusiaux et al., 2010; Haley and Lermusiaux, 2010). Other OA schemes have been used in coastal regions (Hessler, 1984; Stacey et al., 1988; Paris et al., 2002), but without satisfying coastline constraints, in particular, there should be no direct relationship across landforms. In ocean regions with complex 3D geometries, we found that such schemes give field estimates that lead to major issues when used to initialize simulations. Efficient and accurate methodologies for field (e.g. temperature, salinity, biology, and velocity) mapping in complex multiply-connected coastal domains and archipelagos were thus necessary.

The schemes we derive estimate the sea paths between data and model points using the Level Set Method (LSM) and Fast Marching Method (FMM), which are techniques (Sethian, 1999b) to evolve boundaries using appropri-

ate partial differential equations (PDEs). The FMM-based OA methods are shown to be cheaper and more robust than others, in particular than those based on solving diffusion-based PDEs. We also study computational and mathematical properties. We find that higher-order discretizations of the level-set PDEs increase the accuracy of distance estimates, second-order schemes being sufficient for most applications. We show that the covariance matrices are not necessarily positive definite because the Weiner Khinchin and Bochner theorems for positive definiteness, e.g. (Papoulis, 1991), are only valid for convex simply-connected domains. Several approaches to overcome this issue are presented and evaluated. The solutions we propose include introducing a small process noise or, better, reducing the covariance matrix based on the dominant singular value decomposition.

Our new methods are expected to have many applications, in particular to improve the World Ocean Atlas (WOA) climatologies in complex multiply-connected domains. The WOA provides global ocean climatology containing monthly, seasonal and annual means of temperature (T) and salinity (S) fields at standard ocean depths. The temperature and salinity climatologies of the WOA (Levitus, 1982), which is also termed as ‘Levitus Climatology’ and its atlas updates in 1994 (Levitus and Boyer, 1994; Levitus et al., 1994), 1998 (Antonov et al., 1998a,b,c; Boyer et al., 1998a,b,c), 2001 (Stephens et al., 2002; Boyer et al., 2002) and 2005 (Locarnini et al., 2006; Antonov et al., 2006; Garcia et al., 2006a,b), have proven to be valuable tools for studying the hydrographic structures of the World’s oceans. The WOA climatologies have been particularly useful for providing initial and boundary conditions to ocean circulation models. The OA procedure for the ‘Levitus Climatology’ requires the use of an analytical correlation function to determine the covariance (or weight function, as described by Levitus (1982)). If the “straight Euclidean distance” (the straight line distance between two points) is used in such analytical correlation functions, the distance estimate is inappropriate for complex multiply-connected domains, as this “straight Euclidean distance” goes across land and so violates all coastline/bottom constraints. In particular, unconnected water masses are then erroneously blended across landforms, leading to artificial water masses, spurious currents and other fictitious features. The aim of our new methodologies is to satisfy all geometric constraints arising in complex multiply-connected domains and so rectify all of these issues.

The paper is organized as follows. The problems addressed are described in Sect. 2. In Sect. 3, we review the two staged multi-scale statistical

field mapping approach from MSEAS. In Sect. 4, we introduce the new OA methodologies based on the Level Set Method and the Fast Marching Method. An optimization approach for computing the transport streamfunction and total velocity under geostrophic balance by minimizing the unknown inter-island transports is also discussed. The OA approach based on the stochastically forced partial differential equations (SPDE) is introduced in Sect. 5. In Sect. 6, applications of our new methodologies, for the complex regions of Dabob Bay and Philippines Archipelago are presented. In Sect. 7, we study the computational properties of our new mapping schemes. Section 8 consists of a summary and conclusions. The scheme to compute the ‘Levitus Climatology’ maps is summarized in App. A, the FMM algorithm in App. B and the algorithm for minimizing unknown inter-island transports in App. C.

## 2. Problem Statement

We begin by introducing the definitions of convex domains, simply and multiply connected domains. A domain is said to be convex if for every pair of points within the domain, every point on the straight line segment that joins them is also within the domain. A domain is said to be simply-connected if any closed curve within it can be continuously shrunk to a point without leaving the domain. A domain which is not simply-connected is called multiply-connected.

A main research question of this work is field mapping via OAs in complex multiply-connected coastal domains. OA schemes require a description of field statistics which is often provided by analytical correlation functions (Carter and Robinson, 1987; Lam et al., 2009). Such analytical correlation functions are dependent on the spatial separation distance. Using “straight Euclidean” distances in complex multiply-connected domains is not appropriate since there is no direct relationship across landforms. An appropriate measure of distance should be longer. The most straightforward is the length of the shortest sea path i.e., the shortest path without going across complex landforms. Examples of such paths that we computed for the Monterey Bay, Massachusetts Bay, Dabob Bay and Philippines Archipelago are illustrated in Fig. 1. Our new methodology measures these distances most efficiently. It also allows altering distances to account for dynamical or other effects. For example, our estimation of 3D shortest sea paths can be set-up such that vertical distances are weighted more than horizontal ones, hence ac-

counting for effects of reduced correlations across depths. In general, any coordinate system can be used: if instead of depth, density surfaces are employed, diapycnal paths can be weighted more than isopycnal paths. All of these generalizations of the shortest sea path, as well as correlation functions that are constrained by dynamical or feature-based considerations, can be easily accommodated in our new OA methodology.

The physical shortest sea paths, or any generalization of such paths, in complex multiply-connected regions can be efficiently obtained using the following numerical techniques: the Level set method (LSM) (Osher and Sethian, 1988; Sethian, 1999b) and the Fast Marching Method (FMM) (Sethian, 1996, 1999b). These methods model the propagation of evolving boundaries using appropriate PDE's. Here, we illustrate their applications for realistic OAs in both the Philippines Archipelago and Dabob Bay (WA, USA) regions. Other optimization methods for path planning, for example Dijkstra's algorithm (Bertsimas and Tsitsiklis, 1997) and Bresenham-based line algorithm (Bresenham, 1965) could also be used for mapping in complex domains, but we find and show that the FMM and LSM schemes are computationally more efficient and more accurate. We also compare our results to the OA approach based on solving stochastically forced PDEs (Balgovind et al., 1983; Lynch and McGillicuddy, 2001).

The FMM and LSM can also be utilized for estimating the minimum vertical area along any path between two islands. The advantage of the FMM and LSM is that this can be efficiently computed for all island pairs in complex domains with many islands. Such areas are needed to estimate total velocities and transports under a geostrophic constraint (Wunsch, 1996) with our hydrographic OAs. Specifically in our case, these vertical areas are used in the inversion for the transport streamfunction along the island coastlines. The resulting temperature, salinity and velocity field estimates can then be used as first-guess in 3D mapping of primitive-equation fields and error covariances (Lermusiaux et al., 2000; Lermusiaux, 2002).

Mathematical and computational properties of the new mapping schemes are also investigated in detail. To reduce the computational cost and to understand the impact of individual data, sequential processing of observations (Parrish and Cohn, 1985; Cho et al., 1996) is utilized. By definition, the prior covariance matrix should be positive definite. According to the Wiener-Kinchin and Bochner theorem (Papoulis, 1991; Yaglom, 2004; Dolloff et al., 2006), a covariance matrix based on an analytical correlation function will be positive definite if the Fourier transform (or the spectral density of the

correlation function) is non-negative for all frequencies. These theorems are valid only for convex simply-connected domains. In our complex multiply-connected domains, the covariance matrix may become negative due to: a) Numerical errors in the computation of the shortest sea path's length using our new FMM/LSM based schemes, or, b) The presence of landforms. These issues may lead to divergence problems (Brown and Hwang, 1997) in the field mapping. Therefore, the following two questions were investigated and resolved: a) What are the computational errors in the sea path lengths computed using the FMM/LSM and how can they be reduced?, and, b) What are the computational issues including non-positive definite covariances that arise in mapping data in a multiply-connected coastal domain and how can they be remedied? Answering these questions was indispensable for the development of the FMM/LSM based scheme for complex multiply-connected domains.

### 3. MSEAS Objective Analysis Approach

Bayesian-based OA schemes are well established for mapping heterogeneous, multivariate, irregular data (Gandin, 1965; Bretherton et al., 1976; Carter and Robinson, 1987; Daley, 1993) in open oceans, without islands or archipelagos, as well as in atmospheric sciences. Most OA schemes utilize the Gauss-Markov or minimum error variance criterion (Plackett, 1950) to map observations to the numerical grid and they require the computation of Euclidean distances between all data and model points. Within MSEAS, our multi-scale OA scheme consists of the successive utilization of Kalman update steps, one for each scale and for each correlation across scales (Lermusiaux et al., 2000; Lermusiaux, 2002). In particular, our two-scale OA version is summarized in (Lermusiaux, 1997, 1999).

Considering one scale or one interaction between two scales, let us denote the vector of numerical grid point locations as  $\mathbf{x}$  and the vector of measurement locations as  $\mathbf{X}$ , then the OA estimate of the field for that scale or interaction ( $\psi^{\text{OA}}$ ) based on the latest background field ( $\bar{\psi}, \bar{\mathbf{d}}$ ) is given by:

$$\begin{aligned}\psi^{\text{OA}} &= \bar{\psi} + \text{Cor}(\mathbf{x}, \mathbf{X})[\text{Cor}(\mathbf{X}, \mathbf{X}) + \mathbf{R}]^{-1}[\mathbf{d} - \bar{\mathbf{d}}] \\ &= \bar{\psi} + \mathbf{K}^{\text{OA}}[\mathbf{d} - \bar{\mathbf{d}}]\end{aligned}\quad (1)$$

where  $\text{Cor}(\mathbf{x}, \mathbf{X})$  is the correlation matrix between grid and data points (for multivariate OAs or 3D OAs, it is a normalized covariance matrix, see Lermusiaux (2002)),  $\bar{\mathbf{d}} = \mathbf{H}\bar{\psi}$ ,  $\mathbf{H}$  is the observation matrix,  $\mathbf{d}$  is the sensor data

vector,  $\mathbf{R}$  is the error covariance matrix for the sensor data  $\mathbf{d}$  (for the scale considered) at data points, and the gain  $\mathbf{K}^{\text{OA}}$  is given by:

$$\mathbf{K}^{\text{OA}} = \text{Cor}(\mathbf{x}, \mathbf{X})[\text{Cor}(\mathbf{X}, \mathbf{X}) + \mathbf{R}]^{-1} \quad (2)$$

The error covariance of the estimated field (for one scale) is then given by (where  $E[]$  denotes the expectation operator):

$$\begin{aligned} \mathbf{P}^{\text{OA}} &= E[(\mathbf{x} - E[\mathbf{x}])(\mathbf{x} - E[\mathbf{x}])^T] \\ &= \text{Cor}(\mathbf{x}, \mathbf{x}) - \mathbf{K}^{\text{OA}} \text{Cor}(\mathbf{X}, \mathbf{x}). \end{aligned} \quad (3)$$

A comparison between our above update equations for the OA for one scale and the Kalman filter (KF) update equations (using underscore  $t$  to indicate time  $t$  is made in Table 1).

KF Update Equations	MSEAS OA Update equations
hline Kalman gain: $\mathbf{K}_t = \mathbf{P}_{t t-1} \mathbf{H}_t^T \times [\mathbf{H}_t \mathbf{P}_{t t-1} \mathbf{H}_t^T + \mathbf{R}_t]^{-1}$	OA Gain: $\mathbf{K} = \text{Cor}(\mathbf{x}, \mathbf{X}) \times [\text{Cor}(\mathbf{X}, \mathbf{X}) + \mathbf{R}]^{-1}$
State estimate update: $\hat{\mathbf{x}}_t = \hat{\mathbf{x}}_{t t-1} + \mathbf{K}_t (\mathbf{y}_t - \mathbf{H}_t \hat{\mathbf{x}}_{t t-1})$	State estimate update: $\psi^{\text{OA}} = \bar{\psi} + \mathbf{K}[\mathbf{d} - \bar{\mathbf{d}}]$
Error covariance update: $\mathbf{P}_t = (\mathbf{I} - \mathbf{K}_t \mathbf{H}_t) \mathbf{P}_{t t-1}$	Error covariance update: $\mathbf{P}^{\text{OA}} = \text{Cor}(\mathbf{x}, \mathbf{x}) - \mathbf{K}^{\text{OA}} \times \text{Cor}(\mathbf{X}, \mathbf{x})$

Table 1: Comparison between the Kalman Filter and the MSEAS OA update equations (for a univariate variable and one scale).

Thus, if covariances in time are not considered, the update equations of the OA of one scale are equivalent to the update equations of the discrete Kalman filter algorithm. The background error correlation matrix for the field-to-data points,  $\text{Cor}(\mathbf{x}, \mathbf{X})$ , and the background correlation matrix at the data points,  $\text{Cor}(\mathbf{X}, \mathbf{X})$ , are directly related to the KF a priori error covariance matrix  $\mathbf{P}_{t|t-1}$  i.e.  $\text{Cor}(\mathbf{x}, \mathbf{X}) = \mathbf{P}_{t|t-1} \mathbf{H}_t^T$  and  $\text{Cor}(\mathbf{X}, \mathbf{X}) = \mathbf{H}_t \mathbf{P}_{t|t-1} \mathbf{H}_t^T$  ( $\mathbf{H}_t$  is the observation matrix). In 2D horizontal OAs for a single variable, the matrix  $\mathbf{R}$  is often chosen diagonal with a uniform non-dimensional observational error variance  $\sigma_d^2$ , i.e.  $\mathbf{R} = \sigma_d^2 \mathbf{I}$ . In MSEAS, the correlation matrices for a given scale are usually generated from the isotropic function:

$$\text{Cor}(r) = \left(1 - \frac{r^2}{L_0^2}\right) \exp\left[-0.5 \times \left(\frac{r^2}{L_e^2} + \frac{\Delta t^2}{\tau^2}\right)\right] \quad (4)$$

Here,  $\Delta t$  is the difference between the observation and the estimation time and  $\tau$  is the decorrelation time scale. This correlation in time effect extends the direct Kalman update step at a single time to a smoothing OA step using data from different but synoptic times. The parameters  $L_0$  and  $L_e$  are the zero-crossing and the e-folding length scales. The scalar  $r$  is the spatial separation distance.

The MSEAS OAs are often carried out in two stages (Lermusiaux, 1999). In the first stage, the largest dynamical scales (denoted LS) are mapped onto the computational grid using the parameters  $(\tau, L_0, L_e)_{\text{LS}}$ . The background field for this stage is often chosen to be equal to the horizontal mean of all the observations. In the second stage, the smaller scales are mapped using the coefficients  $(\tau, L_0, L_e)_{\text{ME}}$  often corresponding to the most energetic (meso) scales. The background field for this stage is the first stage OA. A major assumption in this OA approach is that the errors in the largest and the most energetic stages are statistically independent. A 3D and dynamics-based extension of this approach, including multiscale interactions, is presented in (Lermusiaux et al., 2000; Lermusiaux, 2002): this 3D multiscale approach also benefits from our new efficient estimation of shortest sea paths. Of course, the accuracy of the field estimates also depends on the spatial and time scale parameters used in the analytical correlation function, as well as on the correlation function itself. The 2D horizontal version of the MSEAS OA has many similarities with the approach used for ‘Levitus Climatology’ maps (Levitus, 1982; Locarnini et al., 2006; Antonov et al., 2006; Garcia et al., 2006a,b) which is described in App. A.

The ‘Levitus Climatology’ and above two-scale MSEAS OA mapping schemes compute the covariance or weight factors by providing Euclidean distances as inputs to correlation functions. If they are not employed in open ocean conditions, actual sea distances between data and model points without going across complex landforms or through bathymetry are needed. The LSM or FMM presented next in Sect. 4 are used to obtain such shortest sea distances between any two points in a complex (e.g. multi-island) multiply-connected coastal region.

#### 4. Methodologies for estimating the length of shortest sea paths in complex coastal regions and archipelagos

The shortest sea paths between data and model-grid points in complex multiply-connected coastal regions are efficiently computed using the LSM

and FMM. These paths are then input to our MSEAS software for multi-scale OAs. The LSM and FMM methods are both more accurate and computationally cheaper than the conventional Bresenham-based line algorithm (Bresenham, 1965) and Dijkstra's algorithm (Bertsimas and Tsitsiklis, 1997). Comparisons to these other algorithms are discussed in (Agarwal, 2009), key results are summarized in Sect. 7.1.

#### 4.1. Objective Analysis using the Level Set Method (LSM)

A level set of a real-valued function  $\phi$  of  $n$  variables is a set of the form:

$$\{(x_1, \dots, x_n) | \phi(x_1, \dots, x_n) = c\} \quad (5)$$

where  $c$  is a constant and  $x_i$  are the  $n$  variables. That is, a level set is the set of points where the function  $\phi$  takes on a given constant value  $c$ .

Osher and Sethian (1988) proposed a numerical technique, which is called the Level Set Method, to implicitly represent and model the propagation of evolving level set interfaces under the influence of a given velocity field using appropriate PDEs. An initial value formulation describing the interface motion is now discussed. The initial position of interfaces are given by level sets of the function  $\phi$ . The evolution of this function  $\phi$  is linked to the propagation of the interface through a time-dependent level set equation. Interfaces can be represented explicitly (parametrized interfaces i.e. interfaces given by  $\mathbf{x} = \mathbf{x}(s)$ , where  $s$  is the parameter) or implicitly (e.g. interfaces given by the zero level set i.e.  $\phi(\mathbf{x}) = 0$ ). Using the implicit representation  $\phi(\mathbf{x})$ , where  $\mathbf{x}$  is the position vector, a convection equation can be solved to propagate level sets advected by a velocity field  $\mathbf{v}$ :

$$\phi_t + \mathbf{v} \cdot \nabla \phi = 0 \quad (6)$$

In many cases, one is interested only in the motion normal to the boundary. Therefore, the velocity  $\mathbf{v}$  can be represented using the scalar speed function  $F$  and the normal direction  $\mathbf{n}$ . Thus.

$$\mathbf{v} = F\mathbf{n} = F \frac{\nabla \phi}{|\nabla \phi|} \quad (7)$$

The hyperbolic, non-linear (Hamilton-Jacobi equation) level set equation, obtained from Eqns. 6 and 7, is given by:

$$\phi_t + F|\nabla \phi| = 0 \quad (8)$$

Integrating the level set equation is an initial value problem which tracks the evolution of the level sets  $\phi=\text{constant}$  assuming  $F$  is given by the specifics of the evolution of the  $\phi$  for a particular problem. The following first order up-winded finite difference approximation can be used to integrate this equation 8 (2-dimensional in space) (Osher and Sethian, 1988; Sethian, 1999b):

$$\phi_{i,j}^{n+1} = \phi_{i,j}^n - \Delta t [\max(F, 0) \nabla_{i,j}^+ + \min(F, 0) \nabla_{i,j}^-]$$

where,

$$\begin{aligned} \nabla_{i,j}^+ &= [\max(D^{-x}\phi_{i,j}^n, 0)^2 + \min(D^{+x}\phi_{i,j}^n, 0)^2 + \\ &\quad \max(D^{-y}\phi_{i,j}^n, 0)^2 + \min(D^{+y}\phi_{i,j}^n, 0)^2]^{1/2} \\ \nabla_{i,j}^- &= [\min(D^{-x}\phi_{i,j}^n, 0)^2 + \max(D^{+x}\phi_{i,j}^n, 0)^2 + \\ &\quad \min(D^{-y}\phi_{i,j}^n, 0)^2 + \max(D^{+y}\phi_{i,j}^n, 0)^2]^{1/2} \end{aligned} \quad (9)$$

Here,  $D^{-x}$  is the first order backward difference operator in the x-direction;  $D^{+x}$  is the first order forward difference operator in the x-direction, etc. Mathematically, these operators are given by:

$$D^{-x}\phi_{i,j} = \frac{\phi_{i,j} - \phi_{i-1,j}}{\Delta x}; \quad D^{+x}\phi_{i,j} = \frac{\phi_{i+1,j} - \phi_{i,j}}{\Delta x} \quad (10)$$

The above numerical technique of the Level Set Method can be used to solve the Eikonal Equation as described next. If the scalar speed function of the front  $F$  is non-negative, then the steady state boundary value problem, known as the Eikonal equation, can be formulated to evaluate the arrival time function  $T(\mathbf{x})$ . The Eikonal equation representing the time  $T(\mathbf{x})$  for the “frontal interface” to reach the position  $\mathbf{x}$  from its initial position is given by:

$$F|\nabla T| = 1 \quad (11)$$

The Eikonal equation simply states that the gradient of the arrival time function is inversely proportional to the local speed of the front. To solve the Eikonal equation, a time dependent problem is proposed. The time evolved steady state solution of the resultant Hamilton-Jacobi equation is the Eikonal equation. Mathematically, this is written as:

$$T_t + F|\nabla T| = 1 \xrightarrow{\text{steady}} F|\nabla T| = 1 \quad (12)$$

This Hamilton-Jacobi equation (Eqn. 12 (Left)) can be discretized using the numerical scheme for the Level Set equation. The steady state solution of this Hamilton-Jacobi equation will be the solution of the Eikonal equation (Eqn. 12 (Right)).

The Level Set Method has been used in a wide variety of applications which include arrival time problems in control theory, generation of minimal surfaces, flame propagation, fluid interfaces, shape reconstruction etc. In the oceanic context, the method can be used to determine shortest sea path lengths as follows. The scalar speed function  $F$  is set to 0 for the grid points on land and 1 for the grid points on water. The level set  $T(\mathbf{x})$ , which is the arrival time function, then also represents the shortest sea distance from the starting position to the position vector  $\mathbf{x}$ . This is because the level set  $T$ , which is the arrival time, when multiplied by the local speed of the front (equal to 1 in this case) gives the level set  $T$  itself for the shortest sea path length estimate. Once these sea distances between all data points and model points are available, the prior correlation functions can be evaluated and the correlation matrices filled in Eqn. 1. An OA can then be computed.

*Operation count for the LSM:* The computation of shortest sea paths via the LSM requires evolving of all the level sets in Eqn. 8 and not simply the zero level set corresponding to the front itself. The LSM thus has an operation count of  $O(N^3)$  in two dimensions for  $N^2$  grid points (Sethian, 1999b). It is computationally expensive since an extra dimension is added to the problem.

A modified approach named ‘Fast Marching level set method’, which significantly reduces the operation count, is described next. Roughly speaking, the two possible ways to obtain steady-state are either iteration towards the solution, or direct construction of the stationary solution  $T$ . While LSM constructs the solution to the Eikonal Eqn. 11 by iterating towards the solution, FMM is based on direct construction of the stationary solution  $T$ .

#### 4.2. Objective Analysis using the Fast Marching Method (FMM)

The Fast Marching Method (FMM) for monotonically advancing fronts has been proposed by Sethian (1996, 1999b). This method leads to a very fast scheme for solving the Eikonal Eqn. 11. The Level set method relies on computing the evolution of all the level sets by solving an initial value PDE using numerical techniques from hyperbolic conservation laws. This is because the Level Set Method iteratively solves the level set equation to

compute the steady state solution which corresponds to the solution of the Eikonal equation (Eqn. 12). As an alternative, an efficient modification is to perform the work only in the neighborhood of the zero level set, as this is known as the ‘narrow band approach’. The basic idea is to tag the grid points as either “alive”, “land mines” or “far away” depending on whether they are inside the band, near its boundary, or outside the band, respectively. The work is performed only on *alive* points, and the band is reconstructed once the land mine points are reached.

The FMM solves boundary value problems without iterations. The method is applicable to monotonically advancing fronts (i.e. the front speed ( $F \geq 0$  or  $F \leq 0$ ) which are governed by the level set equation (Eqn. 12). The steady state form of the level set equation is the Eikonal equation (Eqn. 11) which says that the gradient of the arrival time surface is inversely proportional to the speed of the front. For the two dimensional case, the stationary boundary value problem is given by:

$$|\nabla T|F(x, y) = 1 \quad s.t. \quad \Gamma = \{(x, y) | T(x, y) = 0\} \quad (13)$$

where  $\Gamma$  is the starting position of the interface. The first order finite difference discretization form of the Eikonal equation (Sethian, 1999b) at the grid point (i,j) is given by:

$$[\max(D_{ij}^{-x}T, 0)^2 + \min(D_{ij}^{+x}T, 0)^2 + \max(D_{ij}^{-y}T, 0)^2 + \min(D_{ij}^{+y}T, 0)^2]^{1/2} = \frac{1}{F_{ij}}$$

or,

$$[\max(\max(D_{ij}^{-x}T, 0), -\min(D_{ij}^{+x}T, 0))^2 + \max(\max(D_{ij}^{-y}T, 0), -\min(D_{ij}^{+y}T, 0))^2] = \frac{1}{F_{ij}^2} \quad (14)$$

Equation 14 is essentially a quadratic equation for the value at each grid point (assuming that values at the neighboring nodes are known). An iterative algorithm for computing the solution to Eqn. 14 was introduced by Ruoy and Tourin (1992). FMM is based on the observation that the upwind difference structure of Eqn. 14 means that the information propagates “one way”, i.e. from the smaller values of T to the larger values. Therefore, FMM rests on solving Eqn. 14 by building the solution outward from the smallest time

value  $T$ . The front is swept ahead in an upwind manner by considering a set of points in a *narrow band* around the existing front and bringing new points into the *narrow band* structure. The fast marching algorithm is discussed in detail in App. B (see also (Agarwal, 2009)).

The use of higher-order FMMs (or LSMs) to reduce errors in the estimation of shortest sea path lengths is discussed in Sect. 7.2. They are computationally more expensive but can be necessary for robust and accurate OAs because in complex multiply-connected domains, we found that covariance matrices were sensitive to the accuracy of these lengths. These findings are discussed later in Sections 7.2 and 7.3.

**Operation count for the FMM:** Once again, for estimating the optimal distance, the scalar speed function  $F$  is set to 0 for the grid points on land and 1 for the grid points on water. However, the FMM has a significantly lower operation count of  $O(N^2 \log N)$  for  $N^2$  grid points (Sethian, 1999b). It is computationally much cheaper than the LSM explained above.

The Fast Marching Method, as discussed above, is an efficient way to compute the sea distance between any two locations. These sea distances can then be used for setting up the covariance matrix using any distance-dependent analytical correlation function (e.g. Eqn. 4). Note that the cost of the OAs proper are the same for both the LSM and FMM.

#### 4.3. Total velocity under geostrophic balance: Estimating the minimum vertical area in complex coastal regions and archipelagos

Classically, the synoptic ocean data that are most abundant are hydrographic (temperature and salinity) measurements. If these data are first gridded by OAs, they can be used to estimate a velocity field under the constraint of geostrophic shear (Wunsch, 1996) or other momentum balance assumptions including full momentum conservation of the primitive-equations (Lermusiaux et al., 2000; Lermusiaux, 2002). If geostrophic shear is used as the constraint, to compute transport estimates from the hydrographic OAs, a reference velocity is required. In complex domains, an estimate of the area of the sea cross-sections between any two landforms (e.g. islands) is also often necessary to set the inter-islands transports. The FMM can be directly used to compute the minimum of these cross-sectional areas.

In our case, we utilize an optimization scheme to estimate these inter-island transports, see (Haley et al., 2011; MSEAS, 2010). The scheme is summarized in App. C. Its objective is to find a set of values for the transport streamfunction ( $\Psi$ ) along the island coastlines that produce a suitably

smooth (initial) velocity field, e.g. without unrealistic velocities. If prior estimates of specific transports between islands are known, they are utilized with their uncertainties as inputs to the optimization scheme. If such prior estimates are not available, they are set using a minimum energy principle: a norm of the total velocity between the corresponding islands is minimized under the constraint of geostrophic velocity shear balancing the hydrographic OA maps. To do so, the weight functions require an estimate of the cross-sectional area between islands. This is not easy to compute exactly without a FMM/LSM approach.

With the FMM/LSM schemes, the minimum vertical area can be obtained if we solve the Eikonal Eqn. 11 setting the scalar speed function to be  $F(x,y) = 1/H(x,y)$ . The Eikonal equation thus simplifies to  $|\nabla T| = H$ , which shows that the solution  $T(x,y)$  of this Eikonal equation will be the minimum vertical area. This new approach is used in Sect. 6 to obtain velocity estimates from our hydrographic FMM-based OA maps.

## 5. Objective Analysis using stochastically forced partial differential equations (SPDE's)

Another OA approach that accounts for landforms is based on using SPDE's. The central idea is to represent the underlying field variability as an outcome of a stochastic process using a SPDE where the stochasticity represents the uncertainty in this differential equation. The SPDE is defined only over the sea domain so as to account for geometric constraints. The covariance matrix for the field is then constructed numerically, by solving a set of SPDEs over the sea domain. For example, the stochastically forced Helmholtz equations in 1-D and 2-D in space for the field  $\psi$  in an unbounded domain (Balgovind et al., 1983) are associated with the following covariance functions respectively:

$$\begin{aligned} \frac{\partial^2 \psi}{\partial x^2} - k^2 \psi = \epsilon(x) &\Leftrightarrow C_{\psi\psi}(r) = (1 + kr)e^{(-kr)} \\ \nabla^2 \psi - k^2 \psi = \epsilon(x, y) &\Leftrightarrow C_{\psi\psi}(r) = krK_1(kr) \\ &\simeq \left(\frac{\pi}{2}kr\right)^{1/2} \left(1 + \frac{3}{8kr}\right) e^{-kr} \\ &, kr \rightarrow \infty \end{aligned} \quad (15)$$

where,  $K_1$  is the Bessel function of the second kind. The process noise  $\epsilon$  is a random disturbance with mean 0, standard deviation 1 and no spatial

correlation. Also, the length scale corresponds to the inverse of the SPDE parameter ( $k$ ). Denman and Freeland (1985) and Weaver and Courtier (2001) have proposed other correlation functions which can also be linked to appropriate SPDE's.

A major advantage of this SPDE approach is that the field-to-field covariance  $\text{Cor}(\mathbf{x}, \mathbf{x})$  can be computed numerically from the discretized SPDE along with appropriate boundary conditions (i.e. no flux boundary condition across islands) to directly account for the coastline constraints (Lynch and McGillicuddy, 2001). The discretization of SPDEs (such as Eqn. 15) or any other differential operator defined on the sea domain usually amounts to solving a matrix equation of the form:

$$[A]\{\psi\} = \{e\} \quad (16)$$

where  $\{e\}$  is the spatial discretization of the process noise  $\epsilon$ . All the coastline constraints are then incorporated automatically in this matrix form (16). Since  $[C_{ee}] = [I]$ , the covariance matrices for field-to-field points and field-to-data points are directly obtained from Eqn. 16:

$$\begin{aligned} \text{Cor}(\mathbf{x}, \mathbf{x}) &= [A]^{-1}[C_{ee}][A]^{-T} = ([A]^T[A])^{-1} \\ \text{Cor}(\mathbf{x}, \mathbf{X}) &= [A]^{-1}[C_{ee}][A]^{-T}[H]^T = ([A]^T[A])^{-1}[H]^T \end{aligned} \quad (17)$$

The covariance matrix (17) obtained using the SPDE approach can be used along with Gauss-Markov Estimation theory (see Table 1) to perform OAs in coastal regions. A limitation of this approach is that the resulting fields can be affected by the discretization error associated with the discretized form of the SPDE. In fact, we found that we often need to postprocess (smooth out) the SPDE-gridded fields to remove spurious field gradients. Such gradients, even when small, can lead to spurious velocities by aggregate integration in the vertical for the estimation of total velocity under geostrophic balance. It has also been verified that the SPDE approach is computationally expensive when compared to our new FMM-based methodology.

A similar variant of the above methodology represents the covariance function ( $C_{\psi\psi}$ ), instead of the field ( $\psi$ ), by a SPDE, e.g. a stochastic Helmholtz equation (Logutov, personal communication). The advantage is that the covariances required are then computed directly, without the need of Eqns. 17, which is much cheaper. However, the noise in the resulting OA fields are then found to be even larger (Agarwal, 2009). An heuristic reason is that this simpler representation corresponds to carrying out a “smoothing”

step using the Helmholtz equation only once as compared to twice in the original representation (Eqn. 17). Both of these methods, the SPDE specified for the field ( $\psi$ ) and the SPDE specified for the covariance ( $C_{\psi\psi}$ ) were implemented. They are utilized for comparisons with our new LSM-based and FMM-based schemes.

Even though many different SPDE's could be utilized for mapping a field, in our examples, we selected the stochastically forced Helmholtz equation for three reasons. First, the dynamics of the atmosphere can be approximately governed on the time scale of a few days by a Helmholtz-like equation, which is the equation for the conservation of potential vorticity under the assumptions of a quasi-geostrophic, frictionless, shallow water model without topography (Balgovind et al., 1983; Pedlosky, 1987). Second, a Helmholtz equation can be obtained from the diffusion or wave equations and background correlations are seldom modeled as Gaussian, by solving a pseudo-diffusion equation (Derber and Bouttier, 1999). In these linear PDE's, if the solution is assumed separable in time and space, one obtains for the time variation an ordinary differential equation of the first order. For the spatial variations, one always obtains a Helmholtz equation (Selvadurai, 2000), which is the equation that would be used for spatial mapping. Thirdly, the Helmholtz equation is equivalent to a steady diffusion-reaction equation.

**Operation count for the SPDE-based OAs:** The cost of the SPDE computations of covariances with one data point is at least in  $N^2n$  but most likely in  $N^3$  where  $n$  is the number of time-steps to reach steady state.

Meaningful comparisons among the different methods require comparable covariance parameters. Specifically, for our SPDE-based OA examples using Eqn. 15, the SPDE parameter ( $k$ ) is chosen such that the correlation function corresponding to the stochastically forced Helmholtz equation best fits the analytical correlation function used by our standard OA scheme and by our new LSM or FMM-based schemes, see Sect. 4 and (Agarwal, 2009). The results of these methods can then be compared to each other. This is done next in Sect. 6.2 using the World Ocean Atlas-2005 data in the Philippines Archipelago region.

## 6. Applications illustrating the novel OA methodologies

Methodologies for OAs in complex multiply-connected coastal regions were derived and described in Sect. 4. These methodologies are based on computing optimal sea path lengths using the Level Set Method (LSM) and

the Fast Marching Method (FMM). They efficiently incorporate all geometrical constraints (e.g. there is no direct relationship across landforms) but also other generalized constraints (see Sect. 7). They are utilized next to map temperature, salinity and biological (chlorophyll) fields using a 2-staged mapping scheme in the following regions: Dabob Bay and Philippines Archipelago. For other regions, we refer to Agarwal (2009).

Section 6.1 evaluates our new schemes in Dabob Bay and shows that they are more effective than other classic distance optimizing algorithms such as the Bresenham-based line algorithm (Bresenham, 1965). Section 6.2 compares the different methods introduced in Sects. 4 and 5 for OAs in the Philippines Archipelago region. The estimation of total velocity under geostrophic balance by minimizing unknown inter-island transports is also illustrated.

### 6.1. Objective Analysis in Dabob Bay

Dabob Bay data are used to illustrate the effectiveness of the FMM-based scheme over other distance optimizing algorithms like Bresenham-based line algorithm (Bresenham, 1965). Figure 2 shows maps of temperature and salinity fields obtained using the spatially irregular data in the region and the a. Bresenham-based line algorithm, b. Fast Marching Method. The limitation of Bresenham-based line algorithm is that the optimal distance computed using this method is discontinuous. This results in discontinuities in the covariance and also in the resultant field maps (Agarwal, 2009).

The temperature and salinity field maps (Fig. 2) were obtained using two-scale OAs: one with larger length scales ( $L_0 = 60$ ,  $L_e = 30$ )<sub>LS</sub> and one with smaller length scales ( $L_0 = 30$ ,  $L_e = 15$ )<sub>ME</sub>, in both cases using a non-dimensional observational error variance ( $\sigma_d^2 = 0.25$ ). Temperature and salinity data have higher values in the western arm (Fig. 2 (top)). The eastern arm (Fig. 2 (Middle)) has relatively low temperature and salinity. Effects due to the discontinuity in distance obtained from Bresenham-based line algorithm are clearly evident in Fig. 2 (Middle). Numerical fronts with high temperature and salinity gradients exist at the intersection of the two arms. Such fronts lead to numerical problems in dynamical simulations. The geostrophic velocity obtained using these field maps is unrealistic and has high magnitudes along these fronts. A possible remedy, which reduces the discontinuity effects, is to smooth the distance by averaging distances of neighboring points (Haley, personal communication). We found that this averaging technique becomes numerically very expensive. In addition, the

intensity of erroneous fronts are reduced when this averaged Bresenham-based line algorithm is used, but they still exist. Finally, when our new FMM-based scheme is used to compute distances and to compute the OAs, results are clearly devoid of any numerical fronts (Fig. 2 (bottom)). The FMM-based scheme accurately satisfies the coastline constraints and is computationally inexpensive when compared to the Bresenham-based line algorithms.

## 6.2. Objective Analysis in the Philippines Archipelago

A motivation of this study was the Philippines Straits Dynamics Experiment (PhilEx, Lermusiaux et al. (2011)). In such a complex coastal region, our new schemes were needed to map the very irregular datasets available and initialize simulations. Without them, major problems occurred: neither dynamical studies nor ocean forecasts could be initiated from standard OA schemes. To illustrate this, different OA schemes are compared next, specifically: our new OA methods based on the FMM, a standard OA scheme which ignores islands and uses the direct Euclidean distance, and a stochastically forced PDE scheme (SPDE specified for the field).

The World Ocean Atlas-2005 (Locarnini et al., 2006; Antonov et al., 2006) data for temperature and salinity are used. WOA-05 data are data mapped using the ‘Levitus climatology’ scheme (see App. A) and are regularly spaced. These data are used here primarily to illustrate and discuss the comparison of the different methodologies with a classical data set. Subsequently, synoptic in situ data sets are used for temperature, salinity and biological (chlorophyll) data.

### 6.2.1. Objective Analysis using WOA-05 data: Methods comparison

*Hydrographic field maps.* We compare two-dimensional horizontal OA field maps of the WOA-05 data (Figs. 3-8, Top-Left) computed using schemes presented in Sect. 4 and 5. Figures 3, 4 and 5 show the temperature field maps at the depth of 0m, 200m and 1000m, respectively. Figures 6, 7 and 8 show the salinity field maps at the depth of 0m, 200m and 1000m, respectively. For the two-scale OA schemes, the correlation function used for each scale is given in Eqn. 4. The parameters are: large length scales ( $L_0 = 540$ ,  $L_e = 180$ )<sub>LS</sub>, most energetic length scales ( $L_0 = 180$ ,  $L_e = 60$ )<sub>ME</sub> and observational error variance  $\sigma_d^2 = 0.25$ . For the SPDE approach, the SPDE parameter  $k$  is set to 1/200 (this is a best fit to the correlation function used by the other schemes) and the observational error to  $\sigma_d^2 = 0.25$ .

The OA field maps from all methods (Fig. 3 and 4) indicate that the Philippines Sea and the region near Palawan island is warmer than the rest of the region near the surface (0m, 200m). The region south of the Sulu sea around the Sulu Archipelago has relatively lower temperature. At levels below 500m (see Fig. 5), there is a significant difference in the temperature of the Sulu sea (warm) when compared to the rest of the region (cold) (Gamo et al., 2007; Gordon, 2009). These temperature fields show that direct correlation across landforms are likely weak. Similar observations can be made for Salinity. Salinity in the Sulu Sea and South China Sea (Fig. 6 and 7) is lower than the salinity in the rest of the region near the surface (0m, 200m). At levels below 500m, the salinity in the Sulu Sea (Fig. 8) is significantly lower than in the rest of the region. These salinity fields further support the hypothesis that direct correlation across landforms are weak.

The field maps obtained using the LSM and FMM are identical, but the FMM has a significantly lower computational cost. While the LSM constructs the distance estimate by iterating towards it, the FMM is based on the direct construction of the stationary solution (see Sect. 4). The OA fields obtained using LSM and FMM are very close because the FMM exactly constructs the solution of the discretized Eikonal equation whereas the LSM computes the solution within a desired tolerance limit. Thus, an OA based on FMM should clearly be preferred, as it is more accurate and less expensive. On the other hand, the SPDE approach leads to OAs that are much more noisy than those obtained using the FMM. Since it is also more expensive, the FMM scheme is superior.

The comparison of the different methods for the temperature and salinity maps at 1000m is shown in Figs. 5 and 8, respectively. The methods based on FMM (Figs. 3-8 (Bottom-Left)) and SPDE (Figs. 3-8 (Bottom-Right)) clearly satisfy the coastline constraints. The data in the Sulu Sea, which has high temperature and low salinity compared to the remaining region, does not influence the field outside the Sulu Sea since the two regions are not connected by water at 1000m (assuming only 2D horizontal correlations). On the other hand, the standard OA (Figs. 3-8 (Top-Right)) does not satisfy the coastline constraints. Thus the data outside the Sulu Sea, where the temperature is low and salinity is high, is correlated to the field inside the Sulu Sea. This is undesirable since the direct relationship across landforms is at best very weak. This leads to spurious high temperature and salinity gradients in the Sulu Sea, which creates large spurious geostrophic flow shear. Differences between temperature field maps and salinity field maps

obtained using the FMM and using other OA methods at 1000m are shown in Fig. 9. The differences between the field maps obtained using the FMM and standard OA are large because the standard OA does not incorporate the coastline constraints. There are small differences between field maps obtained using the FMM and SPDE approaches because: i) the SPDE scheme is more sensitive to truncation errors, and ii), the analytical correlation function corresponding to the Helmholtz equation (used in the SPDE approach) is slightly different from the analytical correlation function in the FMM.

The SPDE approach satisfies the coastline constraints, but the discretization errors in the SPDE can be significant and this results in noisy spatial variations in the OA maps, even though this noise is not present in the monthly hydrographic data. This noise then also negatively affects the geostrophic flow shear, and additional smoothing (post-processing) is often needed to filter SPDE-based OA fields. Such post-processing is not required for our FMM-based scheme. As mentioned in Sect. 5, an SPDE approach can be implemented by specifying the SPDE for the field (as shown in Figs 3-8 (Bottom-Right)) or by specifying it directly for the covariance (Logutov, personal communication). The later scheme is a bit cheaper than the former but it is a rough approximation and it further increases the undesired noise of the field maps. Finally, the computational time required by the SPDE approach was confirmed higher than that of the FMM, in accord with the operation counts of Sect. 5. Thus, the FMM appears to be the best among all the methods of Sects. 4 and 5. This was confirmed in many other regions and the FMM scheme is thus used to map the spatially irregular synoptic data in the sections that follow.

*Velocity field maps.* We now illustrate the estimation of total velocity under geostrophic balance in the region using the above OA field maps of hydrographic WOA05 data. The algorithm for optimizing inter-island transports (App. C) is utilized to compute a smooth total flow field estimate under the constraint of geostrophic shear balance. Weight functions based on the minimum vertical area along each pair of islands are computed and used in the algorithm. The estimation of the minimum vertical area has been carried out using the FMM by specifying the scalar speed function in the Eikonal Eqn. 11 as  $F(x,y) = 1/H(x,y)$ , where  $H$  is the ocean depth. The temperature and salinity maps are those of our FMM-based OA scheme (Figs. 3-8 (Bottom-Left)) and of the SPDE approach (Figs. 3-8 (Bottom-Right)), with the Helmholtz equation employed for the field. The streamfunction and velocity fields (at depths 0m, 100m) are shown in Fig. 10. The estimates

based on our FMM-based hydrographic OAs (Fig. 10 (Left)) are in overall good agreement with those obtained using maps based on the stochastically forced Helmholtz equation (Fig. 10 (Right)). However, the SPDE-based velocity fields are noisier, reflecting the spurious noise in the hydrographic OAs. On average, these monthly mean flow estimates suggest larger density-driven velocities in the Mindoro strait, near the Mindanao Island and in the Balabac strait. The maximum absolute velocity, reaches 80 cm/s in the Balabac strait at the surface. At lower depths, velocities remain high in the Mindoro strait and near the Mindanao Island.

Weight functions based on the minimum inter-island distance, which can be obtained using the FMM by specifying the scalar speed function in the Eikonal Eqn. 11 as 1 for sea points and 0 for land points, were also used. The velocity fields obtained using these weight functions had much larger magnitudes, particularly in the Balabac strait (Agarwal, 2009) where the maximum absolute velocity was 141 cm/s. Such high velocity magnitudes are very unlikely. These results show that weight functions based on the minimum vertical area (which is logical for transport estimates) are the most adequate.

#### 6.2.2. Objective Analysis of synoptic data for the Summer 2007

The data used in this example is collected from the Melville exploratory cruise, sg122 and sg126 gliders for the June-July'07 period (Gordon (2009) and Craig Lee, personal communication). The data coverage is shown in Fig. 11 (Top). A portion of the Philippines Archipelago near islands is sampled and OA maps are computed in that region. The scales used are: large length scales ( $L_0 = 1080, L_e = 360$ )<sub>LS</sub> and most energetic length scales ( $L_0 = 270, L_e = 90$ )<sub>ME</sub>. The observational error is set to  $\sigma_d^2 = 0.20$ . The hydrographic field maps obtained using our FMM-based OA scheme are shown in Figs. 12 (Top) and 13 (Top), respectively at depths of 0m and 200m. Once again, these maps clearly indicate that the coastline constraints are appropriately satisfied. At depth of 0m, the warmer regions to the west of Luzon island remain uncorrelated with the Pacific waters east of Luzon. The warm Sibuyan and Visayan Seas can be distinguished from the relatively cold Bohol Sea. At 450m and 1000m, the data in the warm Sulu Sea and Bohol Sea do not impact the other regions: there is no direct relationship across landforms. Similar observations are made for the salinity (e.g. at 0m, the low salinities west of Luzon island do not affect Pacific waters east of Luzon).

### 6.2.3. Objective Analysis for early Winter 2008

The data used in this example is obtained from the joint Melville cruise for the Nov'07-Jan'08 period. The data locations are shown in Fig. 11 (Bottom). The OA parameters are: large length scales ( $L_0 = 1080$ ,  $L_e = 360$ )<sub>LS</sub>, most energetic length scales ( $L_0 = 270$ ,  $L_e = 90$ )<sub>ME</sub> and observational error variance ( $\sigma_d^2 = 0.20$ ). The hydrographic field maps obtained using the FMM-based scheme are shown in Figs. 12 (Bottom) and 13 (Bottom), respectively, at 0m and 200m depth. At the surface, the warm/fresher region west of Luzon is uncorrelated with the region east of Luzon. At depths of 450m and 1000m (not shown), the warm Bohol Sea is enclosed and at these depths, it does not affect other regions either.

Comparing the Winter 2008 from the Summer 20007, the largest differences in temperature and salinity are near the ocean surface (deeper than 200 m depth, fields are much closer). For example, the 0m temperature near Luzon is significantly lower in Winter 2008 than in Summer 2007. However, in the Sulu Sea, the temperature is nearly the same for both Summer 2007 and Winter 2008.

### 6.2.4. Objective Analysis for biological fields (chlorophyll)

Of course, our new FMM-based scheme is not limited to physical fields. Its application to biological fields is illustrated here using the Exploratory cruise Summer 2007 data (Gordon, 2009). Our biological OA field maps (for chlorophyll, nitrate and ammonium) were utilized to initialize coupled physics-biology modeling studies (Burton, 2009; Lermusiaux et al., 2011). The mapping of chlorophyll profiles is illustrated here. The profiles were estimated from satellite images and a region-by-region feature model (Lermusiaux et al., 2011). The biological OA parameters were fit to: large length scales ( $L_0 = 1080$ ,  $L_e = 360$ )<sub>LS</sub>, most energetic length scales ( $L_0 = 270$ ,  $L_e = 90$ )<sub>ME</sub> and observational error variance ( $\sigma_d^2 = 0.20$ ). The resulting chlorophyll maps are illustrated in Fig. 14 at depths of 0m, 10m, 50m, 160m.

The concentration of biological fields like chlorophyll, phytoplankton and zooplankton is substantial near the surface due to the presence of sunlight. The chlorophyll concentration is maximum near islands often driven by winds or bathymetric upwelling. Away from islands, it tends to be more uniform, around a mean value. At 0m and 10m depths, the maximum chlorophyll concentration is observed south of the Visayan sea and in the Bohol Sea. At 50m depth, chlorophyll concentrations remain significant there, but the largest chlorophyll concentrations are observed north of Palawan island. Bi-

ological concentrations at lower depths decrease rapidly.

## 7. Computational Analysis

The computational properties of our methods for mapping irregular data in complex geometries are now described and studied. First, the computational costs are compared in Sect. 7.1. Then, schemes to resolve issues specific to complex multiply-connected coastal regions such as the need for accurate distance estimates (Sect. 7.2) and the need for positive-definite covariance matrices (Sect. 7.3) are discussed. These schemes are important because if the covariance matrix becomes negative, divergence problems occur in the Kalman updates (Brown and Hwang, 1997).

To motivate the computational studies, recall that we generate the covariance matrices using analytical correlation functions defined based on the Euclidean distance. These correlation functions are termed “positive definite” if they generate positive definite covariance matrix in a simply-connected convex domain. It has been well established using the Wiener-Khinchin and Bochner’s theorems that if the Fourier transform (or the spectral density) of a correlation function is non-negative for all frequencies then the correlation function is positive definite (Yaglom, 1987; Papoulis, 1991; Yaglom, 2004; Dolloff et al., 2006). However, we found that for coastal regions, covariance matrices generated from “positive definite correlation functions” may not be positive definite due to: a. numerical errors in the computation of the shortest path lengths using our FMM/LSM schemes, or b. the presence of landforms which lead to multiply-connected or non-convex domains, invalidating assumptions in the Wiener-Khinchin and Bochner theorems (see (Agarwal, 2009) for proof). This can lead to divergence problems in the mapping. Such problems are illustrated using the WOA-05 data (Spliced February and Winter Climatology) shown in Fig. 15 (Top-Left). To simplify, we consider single-scale OAs (all previous example were two-scale OAs). The field maps obtained using our FMM-based scheme with length scales ( $L_0 = 540$ ,  $L_e = 180$ ) and length scales ( $L_0 = 1080$ ,  $L_e = 360$ ) are shown in Fig. 15. Fields obtained using the larger scales (Fig. 15 (Bottom-Left)) clearly show divergence problems near the Palawan island. These problems are not encountered when the smaller length scales are used and are much smaller when a higher-order FMM scheme is used (Fig. 15 (Top-Right)). Questions which motivate our research in Sects. 7.2 and 7.3 are thus: i) What are the computational errors in the shortest sea-path distances com-

puted using the FMM/LSM and how can they be reduced?, and ii) What are the computational issues including non-positive definite covariances that arise in a multiply-connected coastal domain and how can they be remedied? A higher-order FMM than the first-order one (Sect. 4.2) is discussed in Sect. 7.2. Higher-order FMMs significantly reduce errors in the distance estimates, i.e. the difference between the numerically computed and true distance, which limits divergence problems in the mapping. However, even if exact distances are used, when curved boundaries or islands are present in the domain, negative covariances can still occur. Methods to solve these issues are derived in Sect. 7.3.

### 7.1. Comparison of Computational Costs

For all OA schemes, we sequentially process observations (see Parrish and Cohn (1985); Cho et al. (1996); Lermusiaux (1997); Agarwal (2009)). Such sequential processing drastically reduces computational costs and also allows estimating the impact of individual data. Since data are processed sequentially, the costs for the OA schemes are compared by considering a single scalar data point. The main cost is then the computation of the covariance of that data point with all other grid points in the domain. For the FMM, LSM and Dijkstra's schemes, the operation count to do this is driven by the computation of the shortest distances from that data point with all other points. For the SPDE scheme, it depends on the diffusion equation used and on the iterations to reach state-state. For a 2-D domain with  $N$  points in each direction, these operation counts are given in Table 2.

Method	Operation Count
Level Set Method	$O(N^3)$
Fast Marching Method	$O(N^2 \log N)$
SPDE Method	$O(N^2 n)$
Dijkstra's Method	$O(N^3)$

Table 2: Operation counts for computing the covariances among one data point and each of the  $N^2$  model grid points, as obtained using the LSM, FMM, SPDE ( $n$  iterations) and Dijkstra's schemes.

There are a total of  $N^2$  grid points at each level and the operation count for LSM is obtained from an optimistic guess that LSM will take roughly

$N$  steps to converge. In reality, the iterations can take much longer to converge, and the LSM is thus not efficient to compute these distances. On the other hand, FMM is an efficient technique which requires a fast method to locate the smallest value grid point in the *narrow band*. The Min-Heap data structure with backpointers (Sedgewick, 1988) is employed here to efficiently locate the grid point with the minimum value. The total work done in the DownHeap and UpHeap operations, which ensure that the updated quantities do not violate the heap properties, is  $O(\log N)$ . Thus, for a 2D domain with  $N$  grid points in each direction, the FMM has an operation count of  $N^2 \log N$ , which is a significant improvement over the LSM. An efficient SPDE scheme requires at least an order of  $N^2 n$  where  $n$  is the number of iterations to reach steady state. We have observed that the SPDE approach is at least 15% more expensive computationally than the FMM scheme. Thus, the FMM-based scheme is computationally the most efficient.

## 7.2. Higher order Fast Marching Method

In a domain with no islands or landforms, the shortest path length obtained using the FMM/LSM should be equal to the Euclidean distance. But the FMM/LSM have discretization errors which lead to inaccurate length estimates. The Weiner Khinchin and Bochner theorems are valid for covariances computed using the Euclidean distance in a simply-connected convex domain. So, if the domain is simply-connected convex, the covariance matrix can only become negative definite due to the inaccurate length estimates. This may lead to divergence problems in the resultant field maps. In this Section, the goal is to estimate and reduce the computational errors in the shortest path lengths. We first introduce the higher order FMM which reduces these errors.

The FMM scheme presented in Sect. 4.2 is first order, since the first order discretization form (Eqn. 14) of the Eikonal Eqn. 11 is used. A different implementation of FMM with higher accuracy (Sethian, 1999a,b) is discussed here. It employs the second order backward approximation to the first derivative  $T_x$  is given by:

$$T_x \approx \frac{3T_i - 4T_{i-1} + T_{i-2}}{2\Delta x} \Leftrightarrow T_x \approx D^{-x}T + \frac{\Delta x}{2}D^{-x-x}T \quad (18)$$

and the second order forward approximation to the first derivative  $T_x$  given

by:

$$T_x \approx \frac{3T_i - 4T_{i+1} + T_{i+2}}{2\Delta x} \Leftrightarrow T_x \approx D^{+x}T - \frac{\Delta x}{2}D^{+x+x}T \quad (19)$$

Here  $D^{-x}$  and  $D^{+x}$  are the first order forward and backward approximations for the first derivative, respectively (Eqn. 10),  $D^{-x-x} \equiv D^{-x}D^{-x}$  and  $D^{+x+x} \equiv D^{+x}D^{+x}$ .

Consider the switch functions defined by:

$$\begin{aligned} switch_{ij}^{-x} &= \begin{cases} 1 & \text{if } T_{i-2,j} \text{ and } T_{i-1,j} \text{ are known ('Alive')} \\ & \quad \text{and } T_{i-2,j} \leq T_{i-1,j} \\ 0 & \text{otherwise} \end{cases} \\ switch_{ij}^{+x} &= \begin{cases} 1 & \text{if } T_{i+2,j} \text{ and } T_{i+1,j} \text{ are known ('Alive')} \\ & \quad \text{and } T_{i+2,j} \leq T_{i+1,j} \\ 0 & \text{otherwise} \end{cases} \end{aligned} \quad (20)$$

Similar functions are defined in the y-direction. The higher accuracy scheme attempts to use a second order approximation for the derivative whenever the points are tagged as ‘alive’ (the points inside the band where the value of the arrival time function is frozen: see Sect. 4.2) but reverts to the first order scheme otherwise.

The modified discretization equation for the higher accuracy FMM is thus given by:

$$\begin{pmatrix} max([D_{ij}^{-x}T + switch_{ij}^{-x} \frac{\Delta x}{2} D_{ij}^{-x-x}T], \\ -[D_{ij}^{+x}T - switch_{ij}^{+x} \frac{\Delta x}{2} D_{ij}^{+x+x}T], 0)^2 \\ + \\ max([D_{ij}^{-y}T + switch_{ij}^{-y} \frac{\Delta y}{2} D_{ij}^{-y-y}T], \\ -[D_{ij}^{+y}T - switch_{ij}^{+y} \frac{\Delta y}{2} D_{ij}^{+y+y}T], 0)^2 \end{pmatrix} = \frac{1}{F_{ij}^2} \quad (21)$$

It should be noted that the above scheme is not necessarily a second order scheme. Its accuracy depends on how often the switches evaluate to zero and how the number of points where the first order method is applied changes as the mesh is refined. When the number of points where the first order method is applied is relatively small (occurs only near the coastlines), the

error is reduced considerably by using the higher accuracy FMM (Agarwal, 2009). It should also be noted that a third or higher-order approximations for the derivative  $T_x$  can similarly be used to construct more accurate FMM schemes, but this increases the computational cost. We also found that the relative error in the distances computed by the FMM is higher near the data point and it decays as the distance increases. To keep the computational cost low and a uniform relative error, we can thus use higher accuracy FMM near the data points and then progressively shift to the lower order schemes as the distance increases.

The results of using higher order FMMs to minimize errors in the estimation of the shortest path length are illustrated on Fig. 15 (Bottom-Right). They clearly show that the above higher order FMM has attenuated the divergence issues compared to the first order FMM. The divergence issues do not vanish completely because some discretization errors still occur but also because of the presence of landforms. To deal with the latter, which are due to the multiply-connected coastal domains, we further improve schemes next in Sect. 7.3.

### 7.3. Positive Definite covariance matrix for complex multiply-connected coastal regions

Apart from the inaccurate shortest path length, the covariance matrix may also become negative due to the presence of islands and coastlines. This is because the presence of islands and archipelagos stretches the direct Euclidean path, which can render the covariance matrix negative.

For example, consider the idealized multiply-connected domain with an island, shown on Fig. 16. This domain has 12 grid points marked as ocean points and 4 grid points marked as land points. The length of the shortest sea path is computed exactly to form the covariance matrix and so remove all discretization errors of the FMM/LSM. To do so, the positive-definite correlation function  $Cor(r) = \exp\left[-\frac{r^2}{2L^2}\right]$  with  $L=2$  is used. We find that the covariance matrix is not positive definite. The maximum eigenvalue for the covariance matrix is 6.3345 while the minimum is -0.0504. This idealized example clearly reveals that classic Euclidean-based covariance matrices for a complex multiply-connected region may not necessarily be positive definite. This is because the conditions of the Wiener-Khinchin and Bochner's theorems are not satisfied.

One could consider changing the coordinate system, for example curvilinear-

ear coordinates. For adequate coordinate choices, in the transformed space, the domain can then be simply connected and convex. However, the issue then is that the real distances among grid points become position dependent which violates another assumption of the Wiener -Khinchin and Bochner's theorem, see (Agarwal, 2009) for examples and more discussions.

Hence, other schemes have to be used to alleviate the divergence problems (Fig. 17 (Top-Left)) due to the non-positive definite covariance matrix. They include:

- a. **Discarding the problematic data:** Discarding the data that lead to negative values of  $\mathbf{H}_j \mathbf{Cor}(\mathbf{x}, \mathbf{x})_{j-1} \mathbf{H}_j^T$  would solve the issue and eliminate divergences in the resultant OA. However, this method is not adequate since the information in the data is discarded entirely. The field map obtained by discarding the problematic data is shown in Fig. 17 (Top-Right). Clearly, the divergence problems are removed but loosing data is not acceptable.
- b. **Introducing process noise:** Adding a small process noise to the diagonal elements of the covariance matrix would help (Brown and Hwang, 1997), but it will lead to a degree of sub-optimality: the noise affects all of the problematic data. However, it is often a more acceptable scheme than discarding the data. We indeed find that introducing the process noise leads to less divergence problems, as shown in our example, see Fig. 17 (Bottom-Left).
- c. **Dominant Singular Value Decomposition (SVD) of a-priori covariance:** To construct the OA field maps, the full covariance matrix is not required. In fact, the full covariance matrix ( $\mathbf{Cor}(\mathbf{x}, \mathbf{x})$ ) is expensive to compute and store, and it is therefore rarely computed. The necessary requirement for field maps is the covariance matrix among the grid and data points, i.e.  $\mathbf{Cor}(\mathbf{x}, \mathbf{X})$ . The divergence problems can be removed by first obtaining the singular value decomposition (SVD) of  $\mathbf{Cor}(\mathbf{x}, \mathbf{X})$  and then retaining only the dominant singular values and setting the smaller singular values (e.g. less than 1 percent of the maximum singular value) to zero. This SVD procedure renders the covariance matrix non-negative definite, which was verified in multiple examples where a simulated map was used for a true ocean. Based on these results and on minimum error variance arguments, the dominant SVD method is the most acceptable one because it loses the least information contained in the data. Our example is shown on Fig. 17 (Bottom-Right). We find that the field maps obtained using this dominant SVD of the a-priori covariance is free from divergence problems. They are also similar to, but further improve, the fields obtained by introducing the

process noise.

## 8. Summary and Conclusions

New methodologies for the efficient mapping and dynamical inference of ocean fields from irregular data in complex multiply-connected domains were derived and utilized, and computational properties of these mapping schemes were studied. These new OA methods, which satisfy the coastline and bathymetry constraints (e.g. there is no direct relationship across landforms), are based on estimating the length of the optimal sea path using either the Level Set Method (LSM) or the Fast Marching Method (FMM). The optimal sea path was geometrically defined: i.e. for purely horizontal OAs, it is the shortest sea distance in 2D, and for 3D OAs, it is the shortest sea distance in 3D, weighting the vertical or diapycnal distances more than the horizontal ones. Numerical schemes were derived and implemented, and their operation counts compared. Their properties and results were studied in complex domains, the Philippines Archipelago and Dabob Bay, in realistic situations. Both climatological and synoptic datasets were employed and estimates of temperature, salinity and biological (chlorophyll) fields were computed and discussed. We found that without these new OA methods, neither meaningful dynamical studies nor meaningful ocean simulations could be initiated.

Results were compared with those of a standard OA scheme (using across-landforms Euclidean distance in the analytical correlation function), of OA schemes based on other distance estimation methods and of OA schemes based on the use of stochastically forced PDEs (SPDEs). We showed that the FMM-based scheme is computationally cheaper than the LSM-based scheme and diffusion-based SPDE approach. We found that the field maps obtained using our FMM-based schemes were more robust than those obtained using SPDE schemes: fields did not require postprocessing (smoothing), i.e. they were devoid of any spurious gradients. Such spurious gradients in hydrographic maps lead to unrealistic geostrophic flows. The FMM and LSM were the most appropriate for estimating the optimal sea distances among other distance estimation schemes such as Dijkstra's optimization algorithm and the classic Bresenham-based line algorithm. The optimal distance computed using Dijkstra's algorithm is computationally expensive and inaccurate. Apart from being computationally expensive, the optimal distance computed using the Bresenham line algorithm is discontinuous. This results

in the formation of numerical fronts with high field gradients. Such erroneous gradients do not occur when our FMM-based scheme is utilized.

Mathematical and computational properties of the new OA schemes were studied. The sequential processing of observations reduces the computational cost and also helps in understanding the impact of individual data. We found that the use of higher order FMMs increased the accuracy of the estimates of the length of shortest sea paths. The most efficient FMM schemes derived employed a variable order discretization, the order decaying as the distance between the data and model points increases. Accurate FMM distance estimates eliminate one of the sources of negative covariance matrices. The other source is simply the presence of islands or of other non-convex landforms. This is because the Wiener-Khinchin and Bochner theorems are valid only for correlation functions based on the Euclidean distance in convex simply-connected domains. Several approaches to overcome this issue were discussed. These include discarding problematic data points, introducing process noise, and reducing the covariance matrix by applying the dominant singular value decomposition (SVD). Among these, we argued and showed that the latter use of the SVD to reduce the covariance matrix is the best solution.

We have also employed a FMM-based method to estimate the total velocity under geostrophic balance in complex multiply-connected domains. The FMM is used to compute the minimum vertical area between all pairs of islands. These minimum areas are required to compute the transport streamfunction field that optimizes the inter-island transports and produces a smooth velocity field. The result is a mass-conserving geostrophic flow in balance with the hydrographic OA maps and with optimized inter-island transports. This method and the minimum vertical area estimates were necessary to obtain realistic velocity estimates in our Philippines Archipelago examples.

As part of our ongoing work, we have started to incorporate additional geometrical and non-homogeneous dynamical effects to our FMM-based OA scheme. An approach we have followed is to modify the scalar speed function in the Eikonal equation as a function of these geometrical properties and heterogeneous dynamics. In particular, we have utilized a bathymetry-dependent scalar speed function to include bathymetric effects at lower depth levels. To include heterogeneous scales due to the existence of fronts, we can first create an expected length scale field that is a function of space and direction, possibly using raw data only (Agarwal, 2009) or a feature model

(Gangopadhyay and Robinson, 2002). We can then compute the optimal sea path as before, but select the correlation scales as the smallest scales found along that path. For example, if the optimal path crosses a front, the length scale in the across direction would then be the minimum cross-frontal scale. Analogous modification of the scalar speed function or the length scale can be used to incorporate other dynamical effects (e.g. conservation of potential vorticity). In the future, the ideas of optimal path length and our FMM/LSM-based scheme can be used to extend to complex coastal regions our methodology for 3D multivariate and multi-scale spatial mapping of geo-physical fields of their dominant errors (Lermusiaux et al., 2000; Lermusiaux, 2002). Such schemes would be needed for ensemble initializations.

We expect a wide range of applications for our new FMM-based mapping schemes. Already when mapping relatively simple coastal domains, the constraints of landforms are not often accounted for. Constraints due to bathymetric features should also be respected, even in deep ocean regions, from the simpler basins, plateaus and troughs to the more complex sills, ridges, seamounts and trenches. Initial gridded conditions computed by the present FMM methods have already enabled our simulations in varied regions, including the Taiwan region, New England shelf, Dabob Bay and Monterey Bay (Xu et al., 2008; Lermusiaux et al., 2010; Haley and Lermusiaux, 2010). Our new methods would also improve the widely-used gridded ocean databases such as the World Ocean Atlas (WOA) since such oceanic maps were computed without explicitly accounting for coastline and bathymetry constraints.

## 9. Acknowledgments

We are sincerely thankful to Dr. Patrick J. Haley and Wayne G. Leslie for very helpful inputs and multiple discussions. We are thankful to Oleg G. Logutov for sharing his approximate SPDE mapping method. We are very grateful to the whole PhilEx and PLUS teams for their fruitful collaborations. In particular, we thank crews, operators and support personnel of the Melville ship (Prof. Arnold L. Gordon, Lamont-Doherty Earth Observatory of Columbia University), gliders (University of Washington - Applied Physics Laboratory: Craig Lee, Bruce Howe, Marc Stewart) and kayaks (MIT LAMSS group under the guidance of Prof. Henrik Schmidt) for their work and the critical data they provided.

## A. Objective Analysis Schemes of the ‘Levitus Climatology’

The OA schemes used to map the ‘Levitus Climatology’ (Levitus, 1982; Locarnini et al., 2006; Antonov et al., 2006; Garcia et al., 2006a,b) have their origins in the work of Cressman (1959) and Barnes (1964). The approach is based on adding “corrections”, which are computed as a distance-weighted mean of all data point difference values, to the first-guess field. Initially, to reduce the computational time, the World Ocean Atlas 1994 (WOA94) used the Barnes (1973) scheme which requires only a single “correction” to the first-guess field at each grid point in comparison to the successive correction method of Cressman (1959) and Barnes (1964). The most recent WOA98, WOA01 and WOA05 maps were completed employing a three-pass “correction” scheme, using the multi-pass analysis of Barnes (1994). The inputs to this global analysis scheme are differences among a first-guess field and the one-degree square means of the observed data values. An influence radius is then specified and a correction to the first-guess value at all grid points is computed as a distance-weighted mean of only the difference values that correspond to data points that lie within the area defined by the influence radius. Mathematically, the correction factor derived by Barnes (1964) is given by:

$$C_{i,j} = \frac{\sum_{s=1}^d W_s Q_s}{\sum_{s=1}^d W_s} \quad (22)$$

where,

$(i, j)$  - are coordinates of grid points;

$C_{i,j}$  - correction factor at the grid point coordinates  $(i, j)$ ;

$d$  - the number of data points that fall within the area around point  $(i, j)$  defined by the influence radius;

$Q_s$  - difference between the observed mean and the first-guess at the  $s^{th}$  data point in the influence area;

$W_s = \exp(-Er^2/R^2)$  (for  $r \leq R$ ;  $W_s = 0$  for  $r > R$ ) - the correlation weight;

$r$  - distance between data and grid points;

$R$  - influence radius; and,

$E = 4$ .

At each grid point, the final analyzed gridded value  $G_{i,j}$  is the sum of the first guess  $F_{i,j}$  and the correction  $C_{i,j}$ . The expression is:

$$G_{i,j} = F_{i,j} + C_{i,j} \quad (23)$$

If there is no data within the area defined by the influence radius, the correction is zero and the analyzed value is the first-guess. The analysis scheme is set up such that the inference radius can be varied at each iteration. To progressively analyze the smaller scale phenomena with each iteration, the analysis begins with a large inference radius which is decreased gradually with each iteration.

Equation 23 can also be expressed in a matrix-vector form,

$$\mathbf{G} = \mathbf{F} + [\text{diag}(\mathbf{W}\mathbf{e}_d)]^{-1}\mathbf{W}\mathbf{Q} \quad (24)$$

where if  $n$  and  $d$  denote the number of model-grid and data points, respectively, the analyzed field  $\mathbf{G}$  and the first guess  $\mathbf{F}$  are  $n$ -by-1, the correlation weight matrix  $\mathbf{W}$  is  $n$ -by- $d$ , the difference  $\mathbf{Q}$  between the observed mean and first-guess at data points is  $d$ -by-1, and  $\mathbf{e}_d$  is  $d$ -by-1 with unit entities. The operation  $\text{diag}(\mathbf{v})$  creates a diagonal matrix i.e. it puts the vector  $\mathbf{v}$  on the main diagonal.

In analogy to the Kalman Gain ( $\mathbf{K}$ ) from the Gauss Markov criterion ( $\mathbf{K} = \text{Cor}(\mathbf{x}, \mathbf{X})[\text{Cor}(\mathbf{X}, \mathbf{X}) + \mathbf{R}]^{-1}$ ), Equations 24 and 1 show that a similar Gain matrix ( $K_L = [\text{diag}(\mathbf{W}\mathbf{e}_d)]^{-1}\mathbf{W}$ ) can be defined for the Levitus methodology. While the multi-scale OA approach in MSEAS is based on Gauss Markov estimation theory and successive scale-by-scale updates, the Levitus OA is based on computing the distance-weighted mean of all differences between the most recent first-guess field and the data mean within the inference radius and then repeat with a reduced inference radius. The main difference is that Gauss Markov estimation theory requires and uses prior error covariances for the data and the first-guess, while the Levitus OA requires radius of influence estimates and uses data averaging.

## B. Fast Marching Algorithm

The fast marching algorithm (Sethian, 1996, 1999b) is:

1. Initialize
  - (a) *Alive* points: Let  $A$  be the set of all grid points  $(i,j)$  on the starting position of the interface  $\Gamma$ ; set  $T_{ij} = 0$  for all points in  $A$ .
  - (b) *Narrow Band* points: Let the *Narrow Band* be the set of all grid points  $(i,j)$  in the immediate neighborhood of  $A$ ; set  $T_{ij} = \frac{d}{F_{ij}}$  for all points in the *Narrow Band* where,  $d$  is the grid separation distance and  $F$  is the front speed (see Eqn. 13).

- (c) *Far Away* points: Let the *Far Away* region be the set of all remaining grid points  $(i,j)$ ; set  $T_{ij} = \infty$  for all points in the *Far Away* region.

2. Marching Forward

- (a) Begin Loop: Let  $(i_{min}, j_{min})$  be the point in the *Narrow Band* with the smallest value for  $T$ .
- (b) Add the point  $(i_{min}, j_{min})$  to  $A$ ; remove it from the *Narrow Band*.
- (c) Tag as neighbors any points  $(i_{min}-1, j_{min}), (i_{min}+1, j_{min}), (i_{min}, j_{min}-1), (i_{min}, j_{min}+1)$  that are either in the *Narrow Band* or the *Far Away* region. If the neighbor is in the *Far Away* region, remove it from that list and add it to the *Narrow Band*.
- (d) Recompute values of  $T$  at all neighbors in accordance with Eqn. 14. Select the largest possible solution to the quadratic equation.
- (e) Return to the top of the loop.

Here are some properties of the fast marching algorithm. The smallest value in the *Narrow Band* is always correct. Other *Narrow Band* or *Far Away* points with larger values of  $T$  cannot affect the smallest value. Also, the process of recomputing  $T$  values at the neighboring points cannot give a value smaller than any of the accepted value at *Alive points*, since the correct solution is obtained by selecting the largest possible solution to the quadratic equation (Eqn. 14). Thus the algorithm marches forward by selecting the minimal  $T$  value in the *Narrow Band* and recomputing the values of  $T$  at all neighbors in accordance with Eqn. 14.

The key to an efficient version of the algorithm lies in finding a fast way to locate the grid point in the *Narrow Band* with the minimum value for  $T$ . To do so, the heapsort algorithm (Williams, 1964; Sedgewick, 1988) with backpointers is often implemented and it is the algorithm we used here. This sorting algorithm generates a “complete binary tree” with the property that the value at any given parent node is less than or equal to the value at its child node. Heap is represented sequentially by storing a parent node at the location  $k$  and its child at locations  $2k$  and  $2k + 1$ . The member having the smallest value is stored at the location  $k = 1$ .

All *Narrow Band* points are initially sorted in a heapsort. The fast marching algorithm works by first finding, and then removing, the member corresponding to the smallest  $T$  value from the *Narrow Band* which is followed by one sweep of DownHeap to ensure that the remaining elements satisfy the heap property. The DownHeap operation moves the element downwards in

the heap until the new heap satisfies the heap properties. *Far Away* neighbors are added to the heap using the Insert operation which increases the heap size by one and brings the new element to its correct heap location using the UpHeap operation. The UpHeap operation moves the element upwards in the heap until the new heap satisfies the heap properties. The updated values at the neighbor points obtained from Eqn. 14 are also brought to the correct heap location by performing the UpHeap operation.

### C. Estimating the total velocity field under geostrophic balance by minimizing unknown inter-island transports

For mesoscale ocean flows, away from boundary layers, the dominant terms in the horizontal momentum equations are often the Coriolis force and the pressure gradient. Such a flow field, where a balance is struck between the Coriolis and pressure forces, is called geostrophic. The thermal wind equations are obtained for geostrophic flows by assuming that the vertical momentum equation is approximately given by hydrostatic balance. The thermal wind equations are:

$$-f \frac{\partial(\rho v)}{\partial z} = g \frac{\partial \rho}{\partial x} \quad \text{and} \quad f \frac{\partial(\rho u)}{\partial z} = g \frac{\partial \rho}{\partial y} \quad (25)$$

where,  $\rho$  is the density,  $u$  and  $v$  are the horizontal fluid velocity in the zonal (x) and meridional (y) directions respectively, and  $f = 2\Omega \sin\phi$  is the Coriolis parameter at latitude  $\phi$  for the spherical earth rotating at a rate of  $\Omega$ . The thermal wind Eqns. 25 when integrated in the vertical give:

$$\begin{aligned} \rho v(x, y, z, t) &= \frac{-g}{f} \int_{z_0}^z \frac{\partial \rho}{\partial x} dz + \rho v_0 \\ \rho u(x, y, z, t) &= \frac{g}{f} \int_{z_0}^z \frac{\partial \rho}{\partial y} dz + \rho u_0 \end{aligned} \quad (26)$$

where,  $z_0$  is a level of reference where  $v_0, u_0$  are assumed known ( $z_0$  is referred to the level of no motion if  $v_0, u_0 = 0$ ).

Flow estimation based on thermal wind balance (Eqn. 26) is a classical problem in oceanography (Wunsch, 1996). Historically, the main routine measurements were hydrographic: temperature,  $T$ , and salinity,  $S$ , at various depths. The equation of state for seawater then permits the estimation of density at a given pressure from these hydrographic data. Thus, with

Eqn. 26, the vertical shear of the geostrophic flow can be computed from hydrographic data alone and added to a velocity field of reference. This leads to mass-conserving estimates if the reference velocity field is conservative since the geostrophic shear already satisfies continuity. If reference or external barotropic velocities are provided at open boundaries, a Poisson equation can be formed for a transport streamfunction by taking the curl of this barotropic velocity. Solving for the transport streamfunction is then straightforward for domains without any islands. For complex coastal regions with islands, the same Poisson equation can be solved, imposing a fixed transport streamfunction value around each island. The result conserves mass by construction. Details are provided in App. 2.2 of (Haley and Lermusiaux, 2010) for both rigid-lid and free-surface primitive equations.

In the case with islands, a first-guess at the streamfunction along each island coast can be obtained by sinking the islands to a shallow depth, solving for the corresponding streamfunction and averaging its values along each island coast. However, we found that some of the resulting inter-island transports can be unrealistic, often much too large. Hence, Haley et al. (2011) derived a methodology to correct for this. Specifically, they optimize the somewhat known inter-island transports (i.e. add a least-square penalty towards these values) and minimize the unknown ones. These optimized island transport streamfunctions are then used as Dirichlet boundary conditions in the Poisson equation. The result is a mass-conserving geostrophic flow in balance with the hydrographic OA maps and with optimized inter-island transports. This methodology was illustrated in Sect. 6.2.

Summarizing the inter-island transport optimization, the objective is to find a set of constant values for  $(\Psi)$  along the island coastlines that produce a suitably smooth initialization velocity field, e.g. with no unrealistically large velocities. In the unknown straits, the goal is to minimize the kinetic energy or the maximum absolute velocity. The working assumptions are:

1. Coastlines in the given domain can be divided into two distinct subsets:
  - (a). Set A:  $N$  coastlines along which the transport streamfunction is unknown,  $N \neq 0$ .
  - (b). Set B:  $M$  coastlines along which the transport streamfunction is known.
2. A first-guess  $\Psi_0$  exists for the case with coasts in set B, but no coasts in set A, i.e. these coasts and their corresponding interiors are replaced by open ocean (e.g. island sunk to 10m depth).
3. The difference between the first-guess  $\Psi_0$  and the final solution  $\Psi$  is not

extremely large. Otherwise, the information from  $\Psi_0$  would not be accurate enough.

$\Psi_0$  contains useful information such as the position of major currents relative to various coastlines and the effects of topography on the flow. Thus,  $\Psi_0$  can be used to estimate  $\Psi$  along the other island coastlines by constructing an optimization functional for minimizing (in general optimizing) the inter-island transports subject to weak constraints. The optimization functional ( $E$ ) is constructed as follows. Its general form is divided into a summation of three terms, given by:

$$E = E_1 + E_2 + E_3 \quad (27)$$

where,  $E_1$  is the minimizing target for the transport between all pairs of the unknown (Set A) coasts,  $E_2$  is the minimizing target for the transport between all pairs of unknown (Set A) and known (Set B) coasts and  $E_3$  is the minimizing target for the transport between all pairs of the unknown (Set A) coasts and the open boundaries of the domain. The minimum of  $E$  is computed by solving a standard least square problem, i.e. by setting gradients with respect to the unknown  $\Psi$  values equal to zero. These streamfunction values, which smooth the velocity field, are then used as Dirichlet boundary conditions to the final Poisson equation.

The expressions for  $E_1$ ,  $E_2$  and  $E_3$  are provided in Haley et al. (2011). They require the use of appropriate weights:  $w_{nm}$  for the pair of islands denoted here by subscripts  $n$  and  $m$ . These weights are computed using a FMM scheme. Specifically, consider the stream function ( $\Psi$ ) for a two-dimensional horizontal flow. It is defined such that the flow velocity can be expressed as:

$$\vec{u} = (u, v) = -\frac{1}{H} \nabla \times \Psi \hat{k} \Rightarrow u = -\frac{1}{H} \frac{\partial \Psi}{\partial y}, v = \frac{1}{H} \frac{\partial \Psi}{\partial x} \quad (28)$$

Here,  $H$  is the ocean depth. The transport between a pair of islands having streamfunction  $\psi_1$  and  $\psi_2$  is given by:

$$\psi_2 - \psi_1 = \int_A \vec{u} \cdot \hat{n} dA \quad (29)$$

where,  $A$  is the vertical area between the two islands and  $\hat{n}$  is the unit vector normal to the vertical area. Equations 28 and 29 suggest that the appropriate weight function to optimize the velocity field should be  $w_{nm} = 1/A_{nm}^2$ , where,

$A_{nm}$  is the minimum vertical area along any path between the two islands  $n$  and  $m$ . Another heuristic choice of weight function can be  $w_{nm} = 1/d_{nm}^2$ , where the  $d_{nm}$ 's are mean depths. We found this choice only appropriate when the depth is almost uniform in between each pair of islands  $(n, m)$ . In general, this is not the case and we thus needed to compute the minimum areas  $A_{nm}$ . Using the FMM, as described in Sect. 4.2, is a very convenient and efficient way to compute these  $A_{nm}$ 's. Simulations (Agarwal, 2009) have been performed with several other weight functions and they confirmed that the choice of weights  $w_{nm} = 1/A_{nm}^2$  lead to the most accurate flow fields.

## References

Agarwal, A., 2009. Statistical field estimation and scale estimation for complex coastal regions and archipelagos. SM Thesis, Massachusetts Institute of Technology.

Antonov, J. I., Levitus, S., Boyer, T. P., Conkright, M. E., OBrien, T. D., Stephens, C., 1998a. World ocean atlas 1998 volume 1: Temperature of the atlantic ocean. NOAA Atlas NESDIS 27. US Government Printing Office: Washington, DC.

Antonov, J. I., Levitus, S., Boyer, T. P., Conkright, M. E., OBrien, T. D., Stephens, C., 1998b. World ocean atlas 1998 volume 2: Temperature of the pacific ocean. NOAA Atlas NESDIS 28. US Government Printing Office: Washington, DC.

Antonov, J. I., Levitus, S., Boyer, T. P., Conkright, M. E., OBrien, T. D., Stephens, C., 1998c. World ocean atlas 1998 volume 3: Temperature of the indian ocean. NOAA Atlas NESDIS 29. US Government Printing Office: Washington, DC.

Antonov, J. I., Locarnini, R. A., Boyer, T. P., Mishonov, A. V., Garcia, H. E., 2006. World ocean atlas 2005, volume 2: Salinity, s. levitus (ed.). NOAA Atlas NESDIS 62. US Government Printing Office: Washington, DC.

Balgovind, R., Dalcher, A., Ghil, M., Kalnay, E., 1983. A stochastic dynamic model for the spatial structure of forecast error statistics. Monthly Weather Review 111, 701–722.

Barnes, S. L., 1964. A technique for maximizing details in numerical weather map analysis. *Journal of Applied Meteorology* 3, 396–409.

Barnes, S. L., 1973. Mesoscale objective map analysis using weighted time series observations. NOAA Technical Memorandum ERL NSSL-62.

Barnes, S. L., 1994. Applications of the barnes objective analysis scheme, part iii: Tuning for minimum error. *Journal of Atmospheric and Oceanic Technology* 11, 1459–1479.

Bertsimas, D., Tsitsiklis, J. N., 1997. *Introduction to Linear Optimization*. Athena Scientific, Belmont, Massachusetts.

Boyer, T. P., Levitus, S., Antonov, J. I., Conkright, M. E., OBrien, T. D., Stephens, C., 1998a. World ocean atlas 1998 volume 1: Temperature of the atlantic ocean. NOAA Atlas NESDIS 30. US Government Printing Office: Washington, DC.

Boyer, T. P., Levitus, S., Antonov, J. I., Conkright, M. E., OBrien, T. D., Stephens, C., 1998b. World ocean atlas 1998 volume 2: Temperature of the pacific ocean. NOAA Atlas NESDIS 31. US Government Printing Office: Washington, DC.

Boyer, T. P., Levitus, S., Antonov, J. I., Conkright, M. E., OBrien, T. D., Stephens, C., 1998c. World ocean atlas 1998 volume 3: Temperature of the indian ocean. NOAA Atlas NESDIS 32. US Government Printing Office: Washington, DC.

Boyer, T. P., Stephens, C., Antonov, J. I., Conkright, M. E., Locarnini, R. A., OBrien, T. D., Garcia, H. E., 2002. World ocean atlas 2001 volume 2: Salinity, s. levitus (ed.). NOAA Atlas NESDIS 50. US Government Printing Office: Washington, DC.

Bresenham, J. E., 1965. Algorithm for computer control of a digital plotter. *IBM Systems Journal* 4 (1), 25–30.

Bretherton, F. P., Davis, R. E., Fandry, C., 1976. A technique for objective analysis and design of oceanographic instruments applied to mode-73. *Deep-Sea Research* 23, 559–582.

Brown, R. G., Hwang, P. Y. C., 1997. *Introduction to Random Signals and Applied Kalman Filtering*. John Wiley & Sons, United Kingdom.

Burton, L., 2009. Modeling coupled physics and biology in ocean straits. SM Thesis, Massachusetts Institute of Technology.

Carter, E., Robinson, A., 1987. Analysis models for the estimation of oceanic fields. *Journal of Atmospheric and Oceanic Technology* 4 (1), 49–74.

Cho, Y., Shin, V., Oh, M., Lee, Y., 1996. Suboptimal continuous filtering based on the decomposition of the observation vector. *Computers and Mathematics with applications* 32 (4), 23–31.

Cossarini, G., Lermusiaux, P. F. J., Solidoro, C., 2009. The lagoon of venice ecosystem: Seasonal dynamics and environmental guidance with uncertainty analyses and error subspace data assimilation. *Journal of Geophysical Research*, doi:10.1029/2008JC005080.

Cressman, G. P., 1959. An operational objective analysis scheme. *Monthly Weather Review* 87, 329–340.

Daley, R., 1993. *Atmospheric Data Analysis*. Cambridge University Press.

Denman, K. L., Freeland, H. J., 1985. Correlation scales, objective mapping and a statistical test of geostrophy over the continental shelf. *Journal of Marine Research* 43, 517–539.

Derber, J. C., Bouttier, F., 1999. A reformulation of the background error covariance in the ecmwf global data assimilation system. *Tellus A* 51 (2), 195–221.

Dolloff, J., Lofy, B., Sussman, A., Taylor, C., 2006. Strictly positive definite correlation functions. *Proceedings of SPIE* 6235.

Gamo, T., Kato, Y., Hasumoto, H., Kakiuchi, H., Momoshima, N., Takahata, N., Sano, Y., 2007. Geochemical implications for the mechanism of deep convection in a semi-closed tropical marginal basin: Sulu sea. *Deep-Sea Research II* 54, 4–13.

Gandin, L. S., 1965. Objective analysis of meteorological fields. Israel Program for Scientific Translations.

Gangopadhyay, A., Robinson, A. R., 2002. Feature oriented regional modeling of oceanic fronts. *Dynamics of Atmosphere and Oceans* 36 (1-3), 201–232.

Garcia, H. E., Locarnini, R. A., Boyer, T. P., Antonov, J. I., 2006a. World ocean atlas 2005, volume 3: Dissolved oxygen, apparent oxygen utilization, and oxygen saturation, s. levitus (ed.). NOAA Atlas NESDIS 63. US Government Printing Office: Washington, DC.

Garcia, H. E., Locarnini, R. A., Boyer, T. P., Antonov, J. I., 2006b. World ocean atlas 2005, volume 4: Nutrients (phosphate, nitrate, silicate), s. levitus (ed.). NOAA Atlas NESDIS 64. US Government Printing Office: Washington, DC.

Gordon, A. L., 2009. Philex: Regional cruise intensive observational period, leg 1 and 2 reports.

Gordon, A. L., Sprintall, J., Ffield, A., 2011. Regional oceanography of the philippine archipelago. *Oceanography* 24 (1), 14–27.

Haley, P. J., Lermusiaux, P. F. J., 2010. Multiscale two-way embedding schemes for free-surface primitive-equations in the multidisciplinary simulation, estimation and assimilation system. *Ocean Dynamics*, doi:10.1007/s10236-010-0349-4 60, 1497–1537.

Haley, P. J., Lermusiaux, P. F. J., Agarwal, A., 2011. Minimizing the inter-island transport using an optimization methodology. In preparation for *Ocean Modelling*.

Haley, P. J., Lermusiaux, P. F. J., Robinson, A. R., Leslie, W. G., Logoutov, O. G., Cossarini, G., Liang, X. S., Moreno, P., Ramp, S. R., Doyle, J. D., Bellingham, J., Chavez, F., Johnston, S., 2009. Forecasting and reanalysis in the monterey bay/california current region for the autonomous ocean sampling network-ii experiment. *Deep Sea Research II*, doi:10.1016/j.dsr2.2008.08.010 56, 68–86.

Hessler, G., 1984. Experiments with statistical objective analysis techniques for representing a coastal surface temperature field. *Boundary Layer Meteorology* 28, 375–389.

Lam, F. P., Jr., P. J. H., Janmaat, J., Lermusiaux, P. F. J., Leslie, W. G., Schouten, M. W., te Raa, L. A., Rixen, M., 2009. At-sea real-time coupled four-dimensional oceanographic and acoustic forecasts during battlespace preparation 2007. Special issue of the *Journal of Marine Systems* on "Coastal processes: Challenges for Monitoring and Prediction", Drs. J.W. Book, Prof. M. Orlic and Michel Rixen (Guest Eds.), DOI: 10.1016/j.jmarsys.2009.01.029 78, 306–320.

Lermusiaux, P. F. J., 1997. Error subspace data assimilation methods for ocean field estimation: Theory, validation and applications. PhD Thesis, Harvard University.

Lermusiaux, P. F. J., July 1999. Data assimilation via error subspace statistical estimation. part ii: Middle atlantic bight shelfbreak front simulations and esse validation. *Monthly Weather Review* 127, 1408–1432.

Lermusiaux, P. F. J., 2002. On the mapping of multivariate geophysical fields: Sensitivities to size, scales, and dynamics. *Journal of Atmospheric and Oceanic Technology* 19, 1602–1637.

Lermusiaux, P. F. J., 2007. Adaptive modeling, adaptive data assimilation and adaptive sampling. *Physica D* 230, 172–196.

Lermusiaux, P. F. J., Anderson, D. G. M., Lozano, C. J., 2000. On the mapping of multivariate geophysical fields: Error and variability subspace estimates. *Quarterly Journal of the Royal Meteorological Society* 126, 1387–1429.

Lermusiaux, P. F. J., Jr., P. J. H., Leslie, W. G., Agarwal, A., Logoutov, O., Burton, L. J., 2011. Multiscale physical and biological dynamics in the philippines archipelago: Predictions and processes. *Oceanography, Special PhilEx Issue* 24 (1), 70–89.

Lermusiaux, P. F. J., Xu, J., Chen, C. F., Jan, S., Chiu, L. Y., Yang, Y. J., 2010. Coupled ocean-acoustic prediction of transmission loss in a continental shelfbreak region: predictive skill, uncertainty quantification and dynamical sensitivities. *IEEE Transactions, Journal of Oceanic Engineering*, doi: 10.1109/JOE.2010.2068611 35 (4), 895–916.

Levitus, S., 1982. Climatological atlas of the world ocean. NOAA Professional Paper 13. US. Government Printing Office: Washington,DC.

Levitus, S., Boyer, T. P., 1994. World ocean atlas 1994: Volume 4: Temperature. NOAA Atlas NESDIS 4. US Government Printing Office: Washington, DC.

Levitus, S., Burgett, R., Boyer, T. P., 1994. World ocean atlas 1994, volume 3: Salinity. NOAA Atlas NESDIS 3. US Government Printing Office: Washington, DC.

Locarnini, R. A., Mishonov, A. V., Antonov, J. I., Boyer, T. P., Garcia, H. E., 2006. World ocean atlas 2005, volume 1: Temperature, s. levitus (ed.). NOAA Atlas NESDIS 61, U.S. Government Printing Office: Washington, D.C.

Logoutov, O. G., 2008. A multigrid methodology for assimilation of measurements into regional tidal models. *Ocean Dynamics*, doi:10.1007/s10236-008-0163-4 58, 441–460.

Logoutov, O. G., Lermusiaux, P. F. J., 2008. Inverse barotropic tidal estimation for regional ocean applications. *Ocean Modelling*, doi:10.1016/j.ocemod.2008.06.004 25, 17–34.

Lynch, D. R., McGillicuddy, D. J., January 2001. Objective analysis for coastal regimes. *Continental Shelf Research* 21, 1299–1315.

MSEAS, 2010. The multidisciplinary simulation, estimation, and assimilation systems (<http://mseas.mit.edu/>. <http://mseas.mit.edu/codes>). Reports in Ocean Science and Engineering 6, Department of Mechanical Engineering, Massachusetts Institute of Technology, Cambridge.

Osher, S., Sethian, J. A., 1988. Fronts propagating with curvature-dependent speed: algorithms based on hamilton-jacobi formulations. *Journal of Computational Physics* 79 (1), 12–49.

Papoulis, A., 1991. Probability, Random Variables and Stochastic Processes. McGraw-Hill.

Paris, C. B., Cowen, R. K., Lwiza, K. M. M., Wang, D. P., Olson, D. B., 2002. Multivariate objective analysis of the coastal circulation of barbados, west indies: implication for larval transport. *Deep-Sea Research I* 49, 1363–1386.

Parrish, D. F., Cohn, S. E., 1985. A kalman filter for a two-dimensional shallow-water model: Formulation and preliminary experiments. Office Note 304, U.S. Department of Commerce, NOAA, NWS, NMC.

Pedlosky, J., 1987. Geophysical Fluid Dynamics. Springer.

Plackett, R. L., 1950. Some theorems in least squares. *Biometrika* 37 (1-2), 149–157.

Ruoy, E., Tourin, A., 1992. A viscosity solutions approach to shape from shading. *SIAM Journal on Numerical Analysis* 29, 867–884.

Sedgewick, R., 1988. Algorithms. Addison-Wesley.

Selvadurai, A. P. S., 2000. Partial Differential Equations in Mechanics. Springer.

Sethian, J. A., 1996. A fast marching level set method for monotonically advancing fronts. *Proceedings of the National Academy of Sciences* 93 (4), 1591–1595.

Sethian, J. A., 1999a. Fast marching methods. *SIAM Review* 41 (2), 199–235.

Sethian, J. A., 1999b. Level Set Methods and Fast Marching Method. Cambridge University Press, Cambridge, United Kingdom.

Stacey, M. W., Pond, S., LeBlond, P. H., 1988. An objective analysis of the low-frequency currents in the strait of georgia. *Atmosphere-Ocean* 26 (1), 1–15.

Stephens, C., Antonov, J. I., Boyer, T. P., Conkright, M. E., Locarnini, R. A., OBrien, T. D., Garcia, H. E., 2002. World ocean atlas 2001 volume 1: Temperature, s. levitus (ed.). NOAA Atlas NESDIS 49. US Government Printing Office: Washington, DC.

Weaver, A., Courtier, P., 2001. Correlation modelling on the sphere using a generalized diffusion equation. *Quarterly Journal of the Royal Meteorological Society* 127, 1815–1846.

Williams, J. W. J., 1964. Algorithm 232 - heapsort. *Communications of the ACM* 7 (6), 347348.

Wunsch, C., 1996. The Ocean Circulation Inverse Problem. Cambridge University Press, Cambridge, United Kingdom.

Xu, J., Lermusiaux, P. F. J., Haley, P. J., Leslie, W. G., Logoutov, O. G., 2008. Spatial and temporal variations in acoustic propagation during the plusnet07 exercise in dabob bay. Proceedings of Meetings on Acoustics (POMA), 155th Meeting Acoustical Society of America, doi: 10.1121/1.2988093 4.

Yaglom, A. M., 1987. Correlation theory of stationary and related random functions I. Springer-Verlag.

Yaglom, A. M., 2004. An Introduction to the Theory of Stationary Random Functions (Dover Phoenix Editions). Dover.

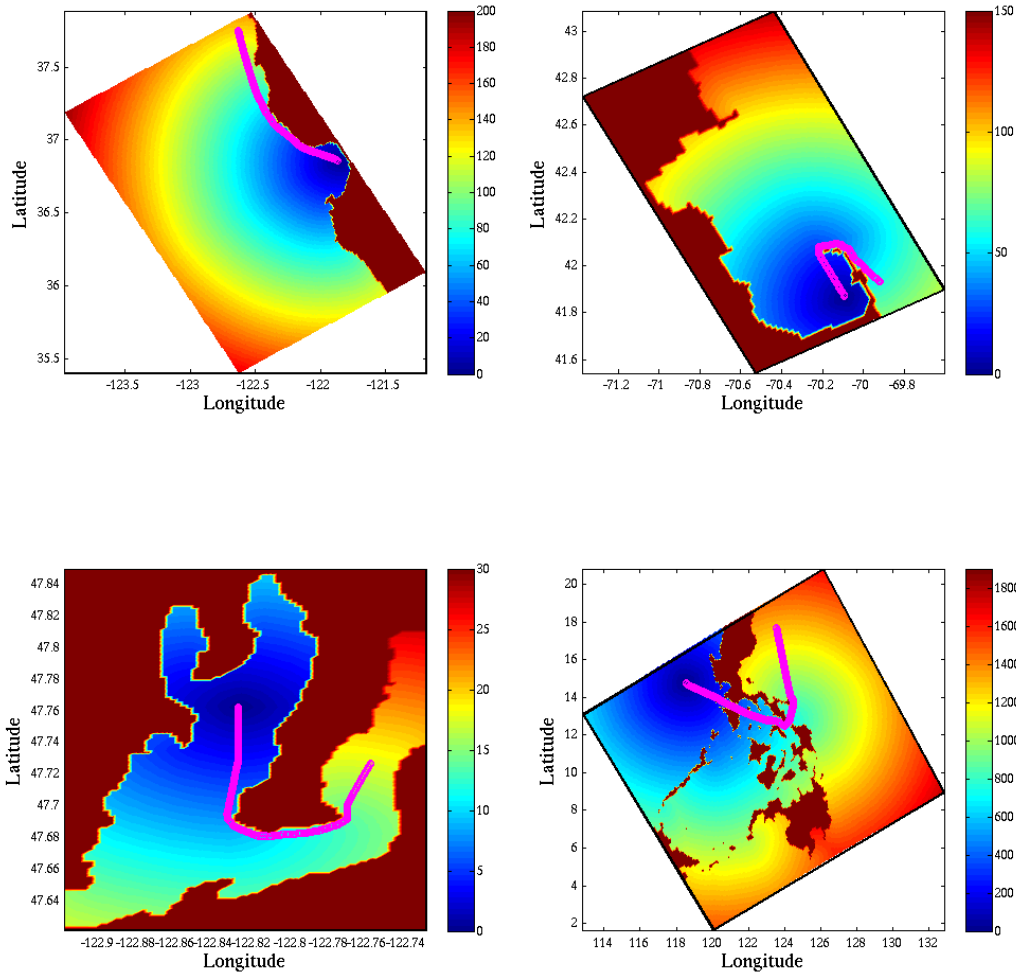


Figure 1: Examples of optimal shortest sea paths computed using the Level Set Method in: (Top - Left) Monterey Bay; (Top - Right) Massachusetts Bay; (Bottom - Left) Dabob Bay; (Bottom - Right) Philippines Archipelago.

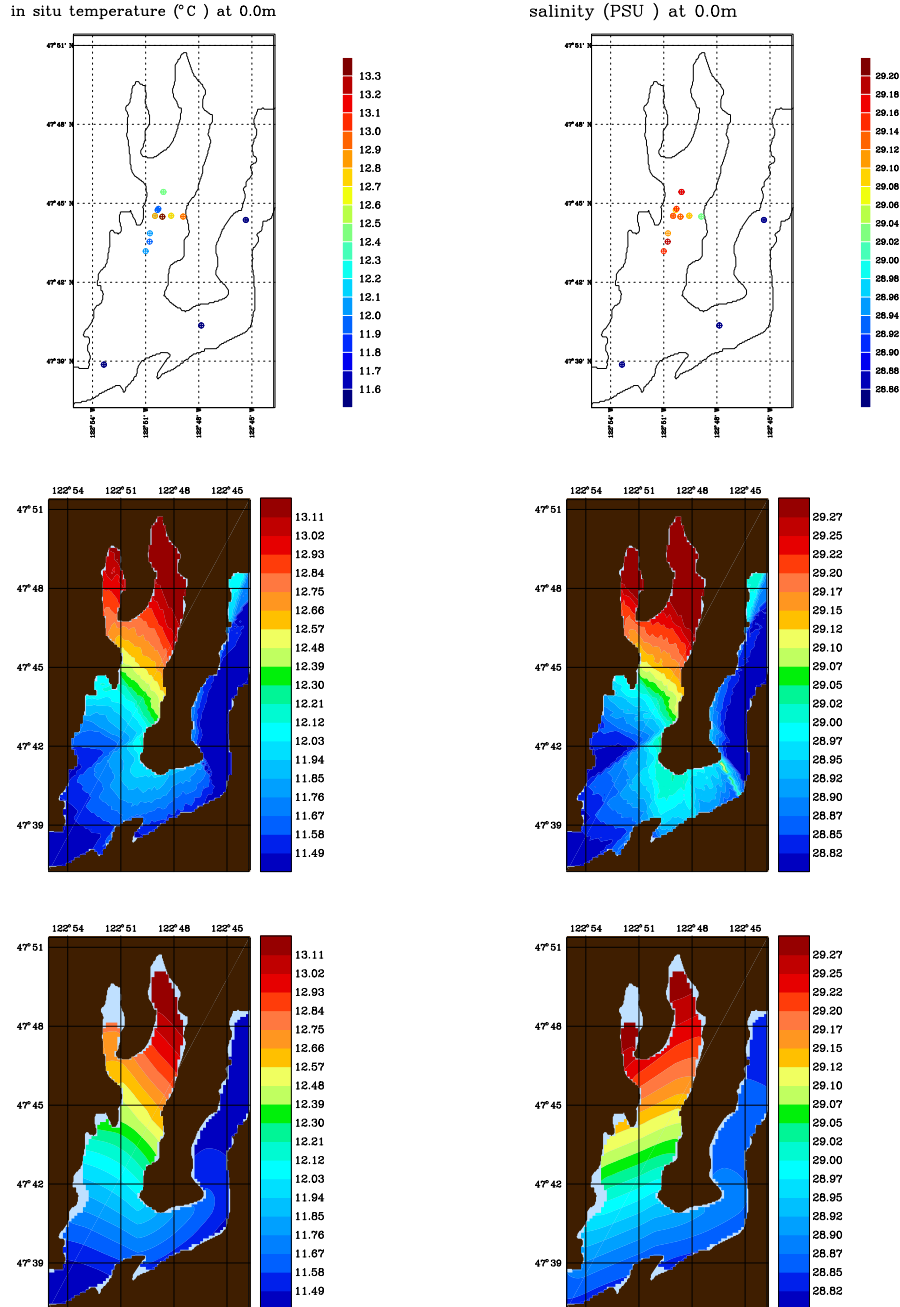


Figure 2: Temperature (°C) (Top - Left) and Salinity (PSU) (Top-Right) data in Dabob Bay. OA fields for this Temperature (°C) (Left) and Salinity (PSU) (Right) in Dabob Bay from the optimal path length computed using: (Middle) Bresenham-based line algorithm; (Bottom) Fast Marching Method, clearly showing the issues of the Bresenham-based line algorithm.

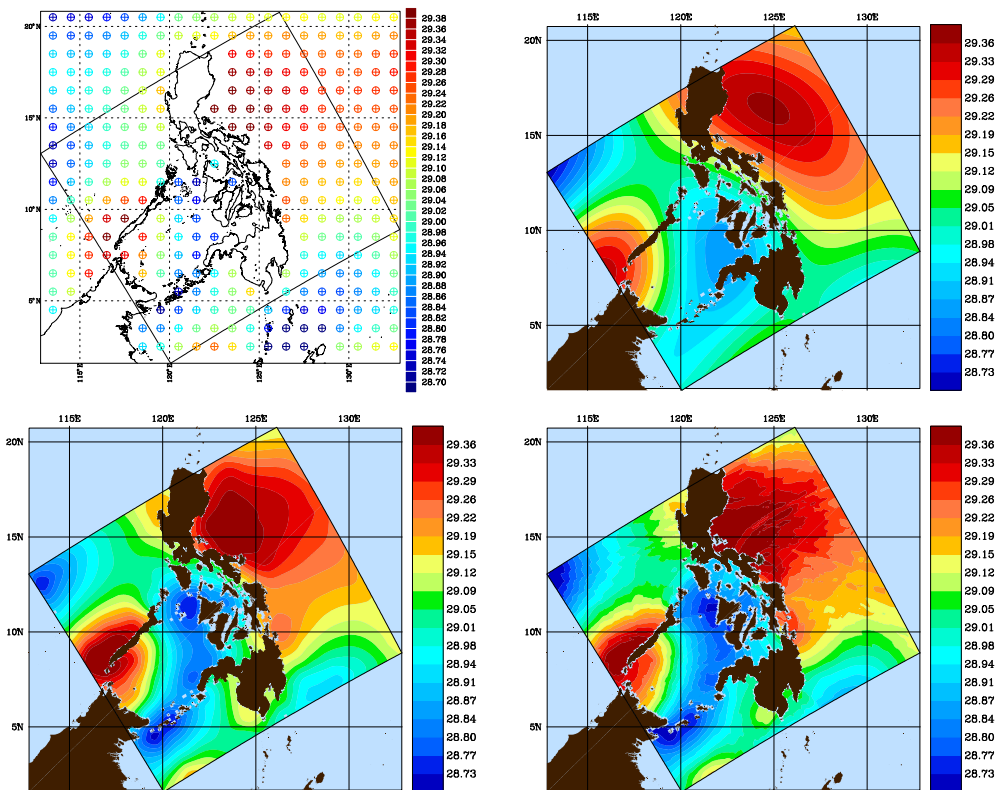


Figure 3: (Top - Left) World Ocean Atlas 2005 Climatology in situ temperature ( $^{\circ}\text{C}$ ) at 0m. Temperature ( $^{\circ}\text{C}$ ) OA Fields obtained using: (Top - Right) Standard OA without taking islands into account; (Bottom - Left) Fast Marching Method; (Bottom - Right) SPDE approach (representing field by a stochastically forced Helmholtz Equation).

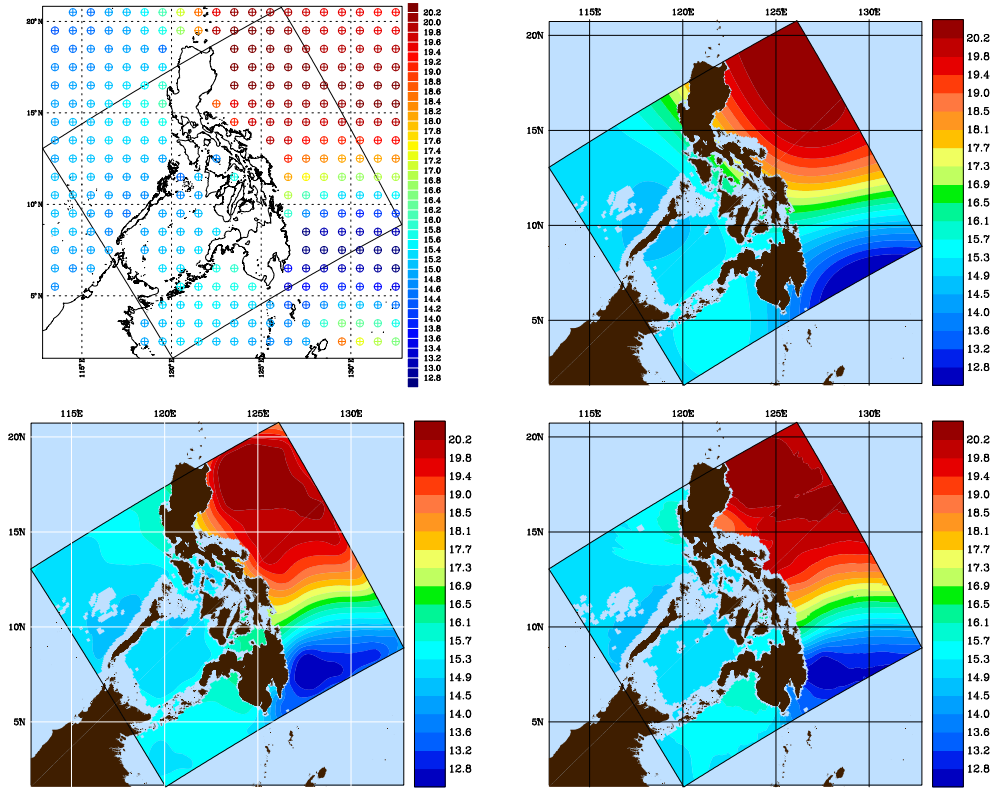


Figure 4: (Top - Left) World Ocean Atlas 2005 Climatology in situ temperature ( $^{\circ}\text{C}$ ) at 200.0m. Temperature ( $^{\circ}\text{C}$ ) OA Fields obtained using: (Top - Right) Standard OA without taking islands into account; (Bottom - Left) Fast Marching Method; (Bottom - Right) SPDE approach (representing field by a stochastically forced Helmholtz Equation).

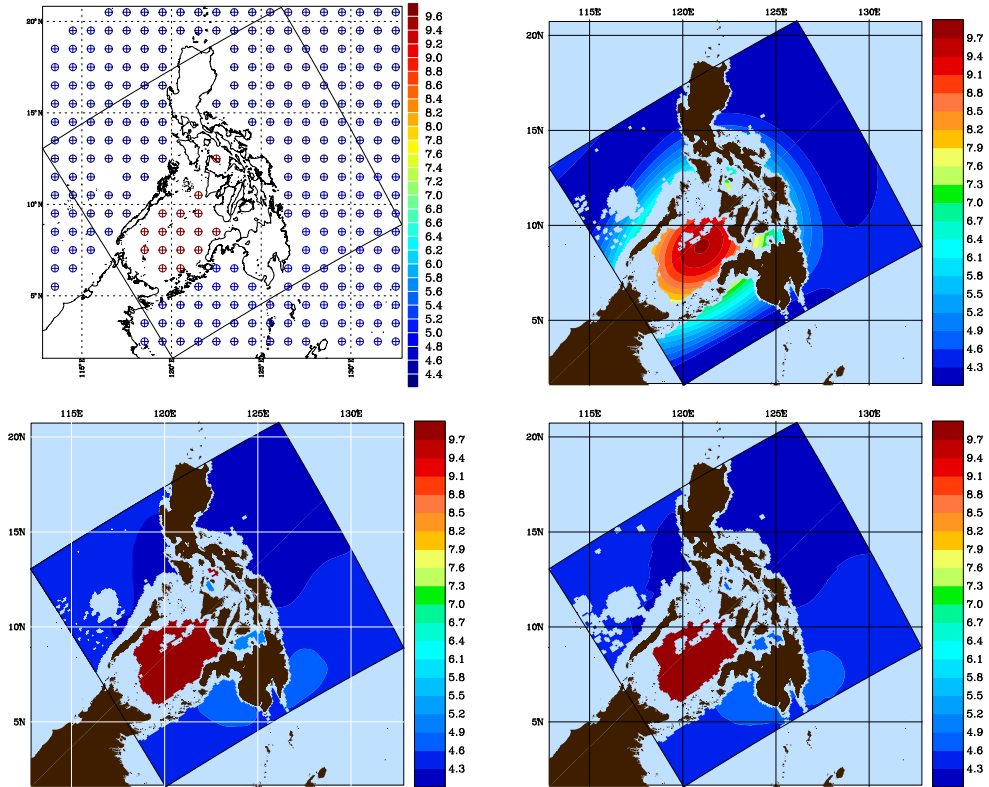


Figure 5: (Top - Left) World Ocean Atlas 2005 Climatology in situ temperature ( $^{\circ}\text{C}$ ) at 1000.0m. Temperature ( $^{\circ}\text{C}$ ) OA Fields obtained using: (Top - Right) Standard OA without taking islands into account; (Bottom - Left) Fast Marching Method; (Bottom - Right) SPDE approach (representing field by a stochastically forced Helmholtz Equation).

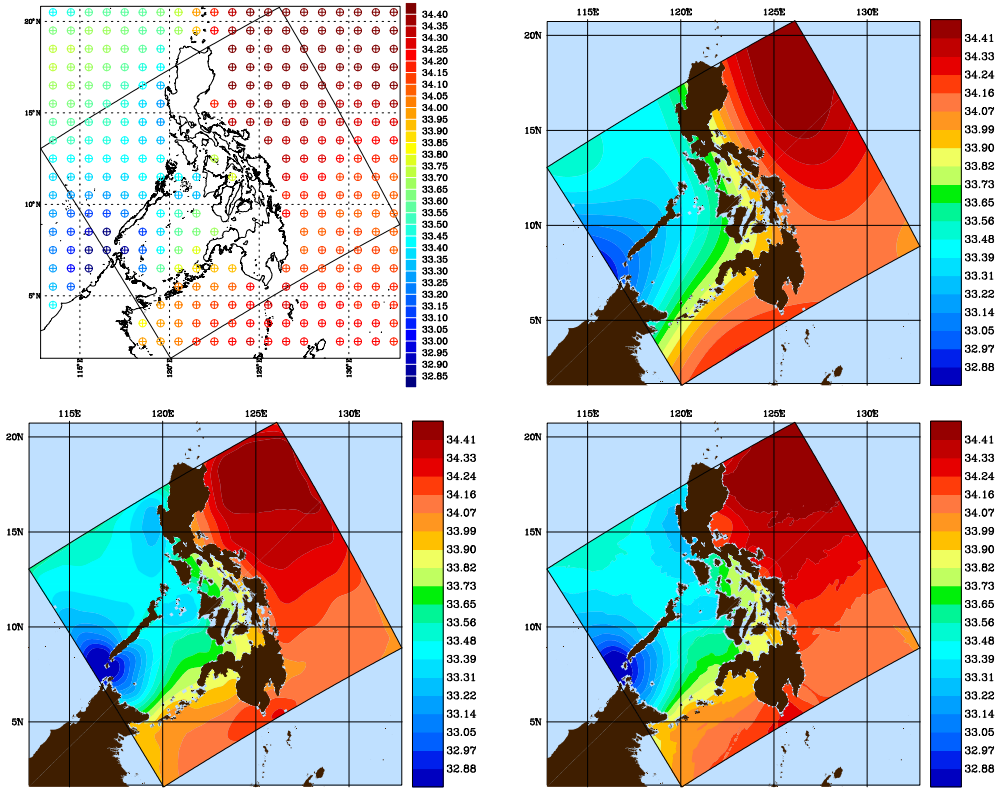


Figure 6: (Top - Left) World Ocean Atlas 2005 Climatology in situ Salinity (PSU) at 0m. Salinity (PSU) OA Fields obtained using: (Top - Right) Standard OA without taking islands into account; (Bottom - Left) Fast Marching Method; (Bottom - Right) SPDE approach (representing field by a stochastically forced Helmholtz Equation).

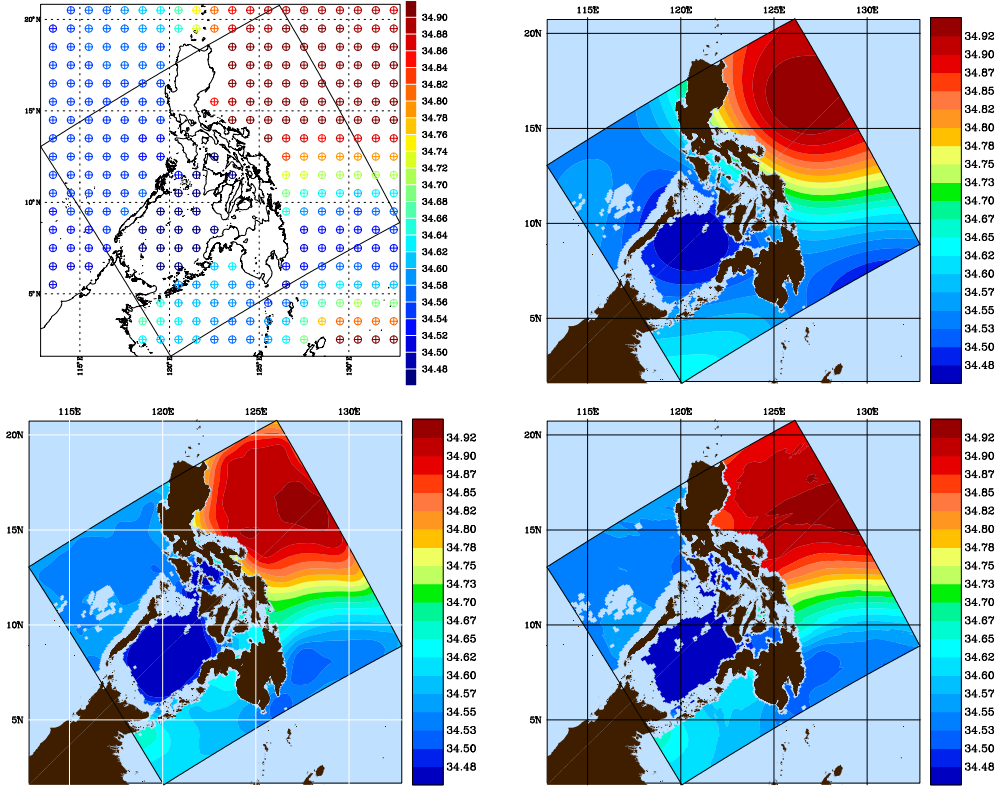


Figure 7: (Top - Left) World Ocean Atlas 2005 Climatology in situ Salinity (PSU) at 200.0m. Salinity (PSU) OA Fields obtained using: (Top - Right) Standard OA without taking islands into account; (Bottom - Left) Fast Marching Method; (Bottom - Right) SPDE approach (representing field by a stochastically forced Helmholtz Equation).

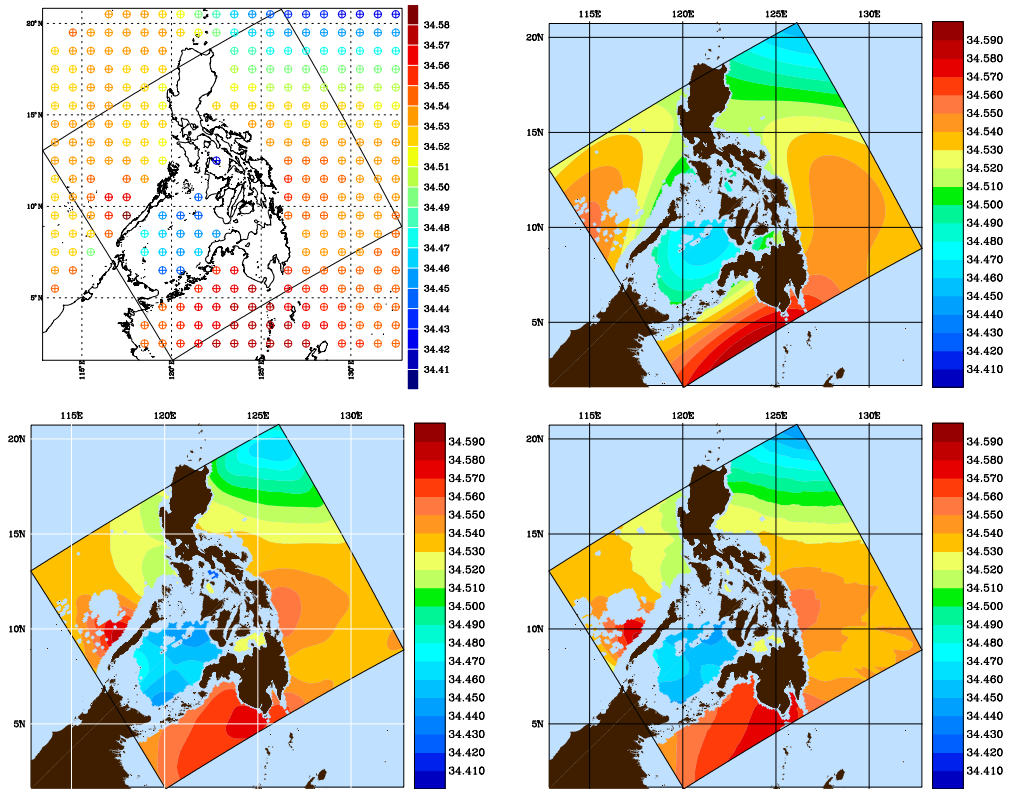


Figure 8: (Top - Left) World Ocean Atlas 2005 Climatology in situ Salinity (PSU) at 1000.0m. Salinity (PSU) OA Fields obtained using: (Top - Right) Standard OA without taking islands into account; (Bottom - Left) Fast Marching Method; (Bottom - Right) SPDE approach (representing field by a stochastically forced Helmholtz Equation).

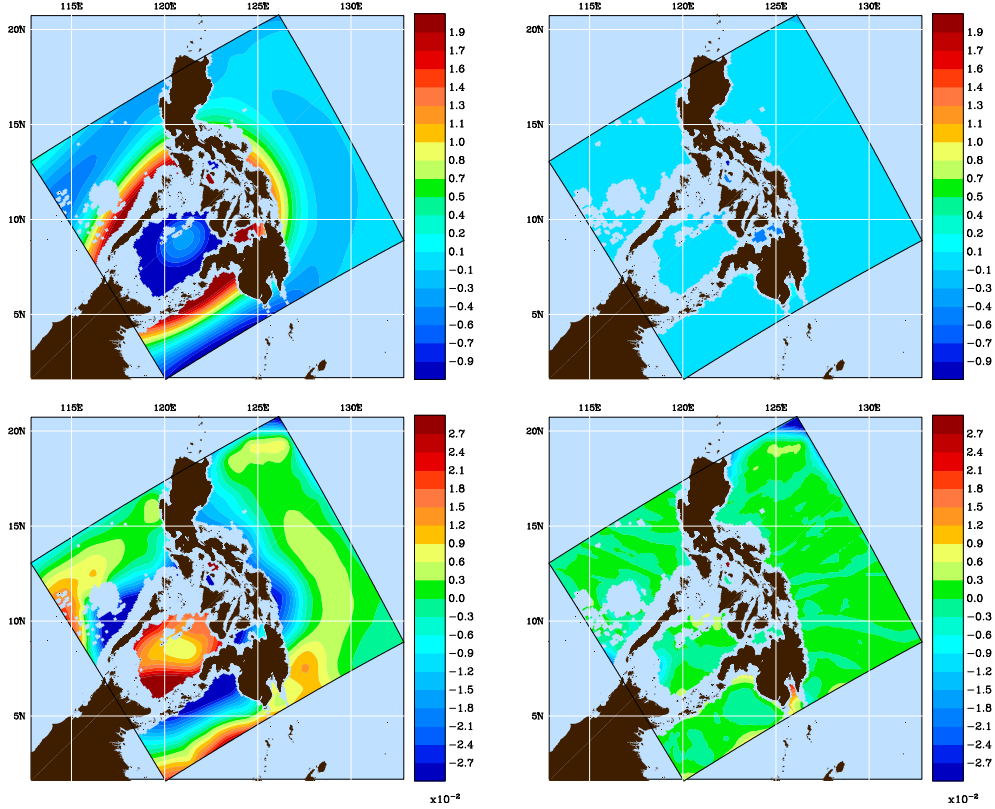


Figure 9: Difference between Temperature ( $^{\circ}\text{C}$ ) field at Level = 1000m obtained using Fast Marching Method and using: (Top - Left) Standard OA; (Top - Right) SPDE (representing field by Helmholtz equation). Difference between Salinity (PSU) field at Level = 1000m obtained using Fast Marching Method and using: (Bottom - Left) Standard OA; (Bottom - Right) SPDE (representing field by Helmholtz equation).

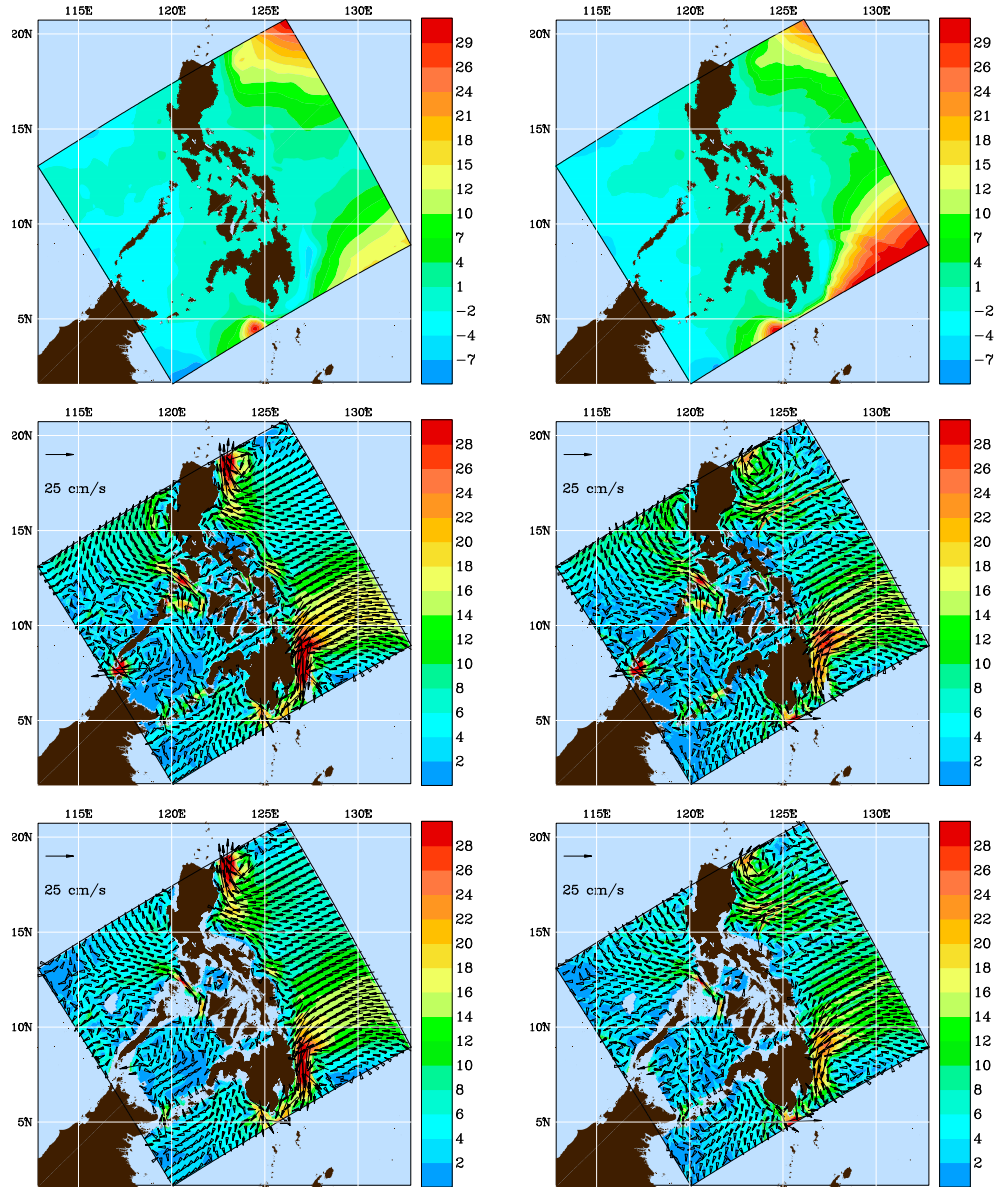
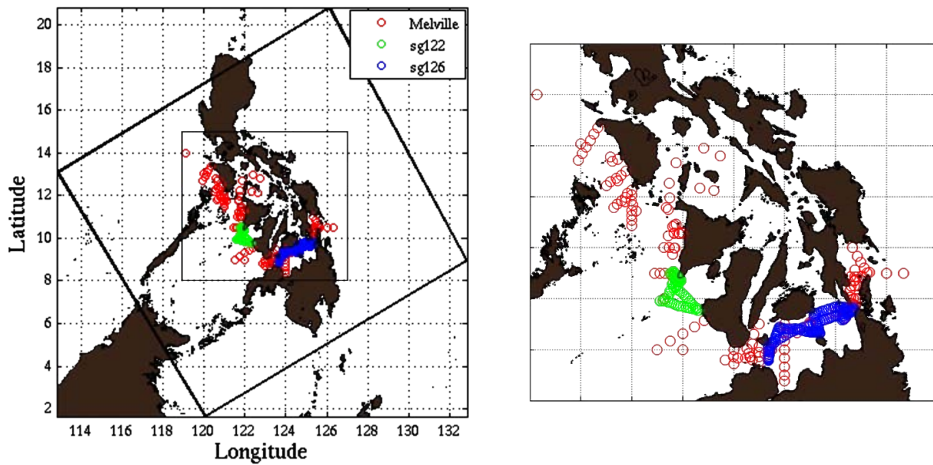


Figure 10: Velocity estimation under geostrophic balance and optimized inter-island transports (weight functions based on the minimum vertical area) from hydrographic field maps (WOA05) obtained using the FMM (Left) and using the SPDE Approach (Right): (Top) Streamfunction, Velocity at depths: (Middle) 0m; (Bottom) 100m.

Summer 2007

Exploratory cruise data collected from June-July, 07



Winter 2008

PHILEX - Joint Cruise - Melville Data

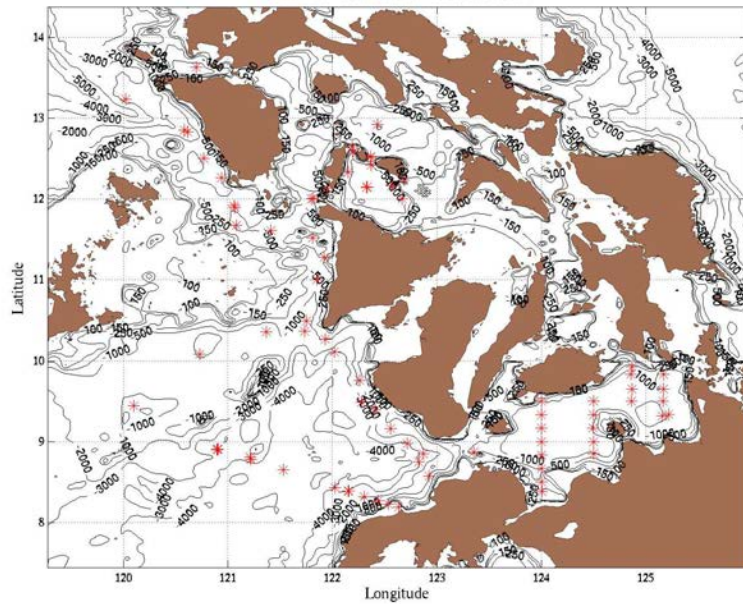
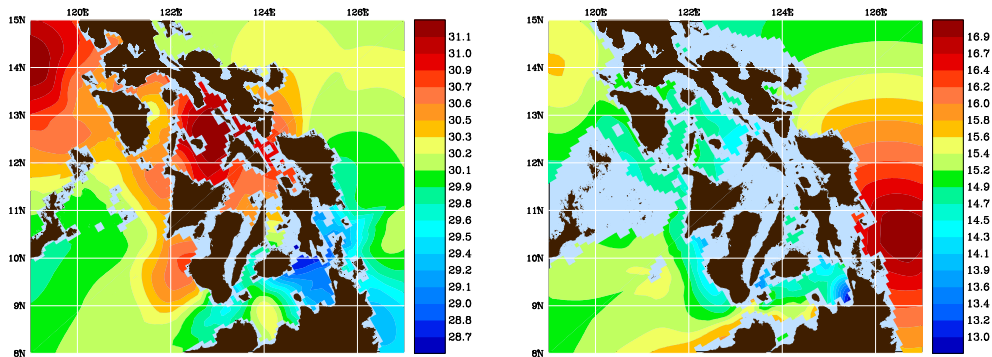


Figure 11: Locations of: (Top) Melville exploratory cruise and glider data (Summer 2007) and (Bottom) Melville joint cruise Data (Winter 2008), both in the Philippines Archipelago.

Summer 2007



Winter 2008

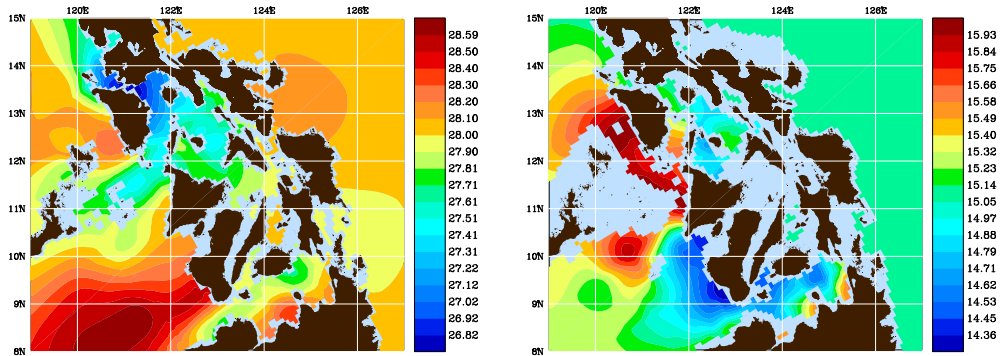
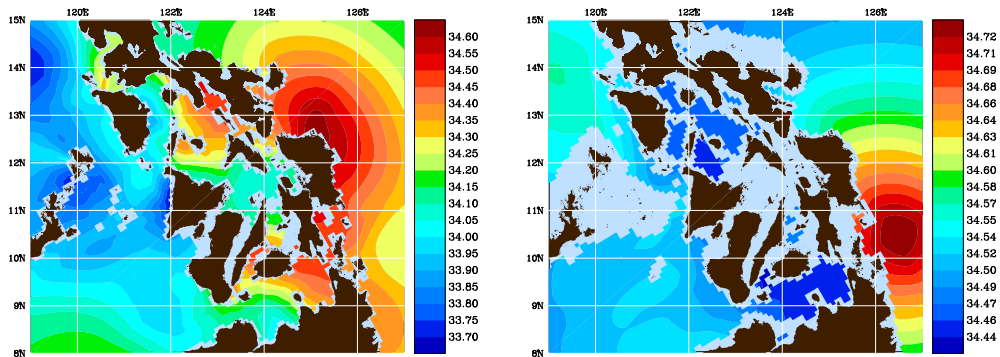


Figure 12: Temperature ( $^{\circ}\text{C}$ ) OA Fields at 0m (Left) and 200m (Right) using the: (Top) Melville exploratory cruise and glider data (Summer 2007); (Bottom) Melville joint cruise data (Winter 2008). Colorbars are not the same for the two periods due to the winter and summer variability.

Summer 2007



Winter 2008

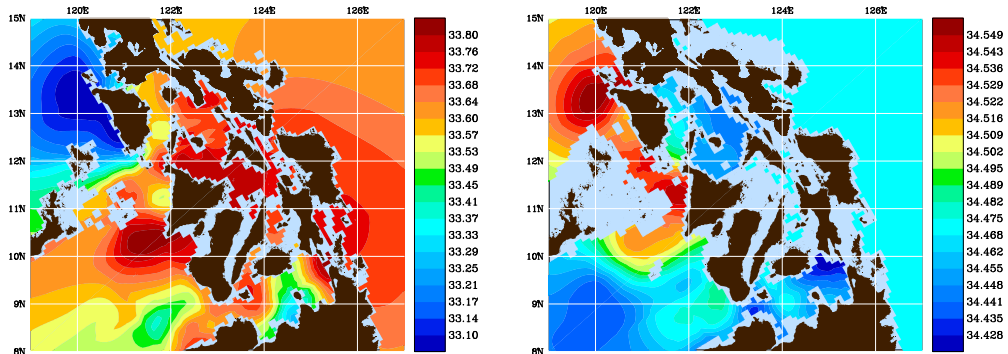


Figure 13: Salinity (PSU) OA Fields at 0m (Left) and 200m (Right) using the: (Top) Melville exploratory cruise and glider data (Summer 2007); (Bottom) Melville joint cruise data (Winter 2008). Colorbars are not the same for the two periods due to the winter and summer variability.

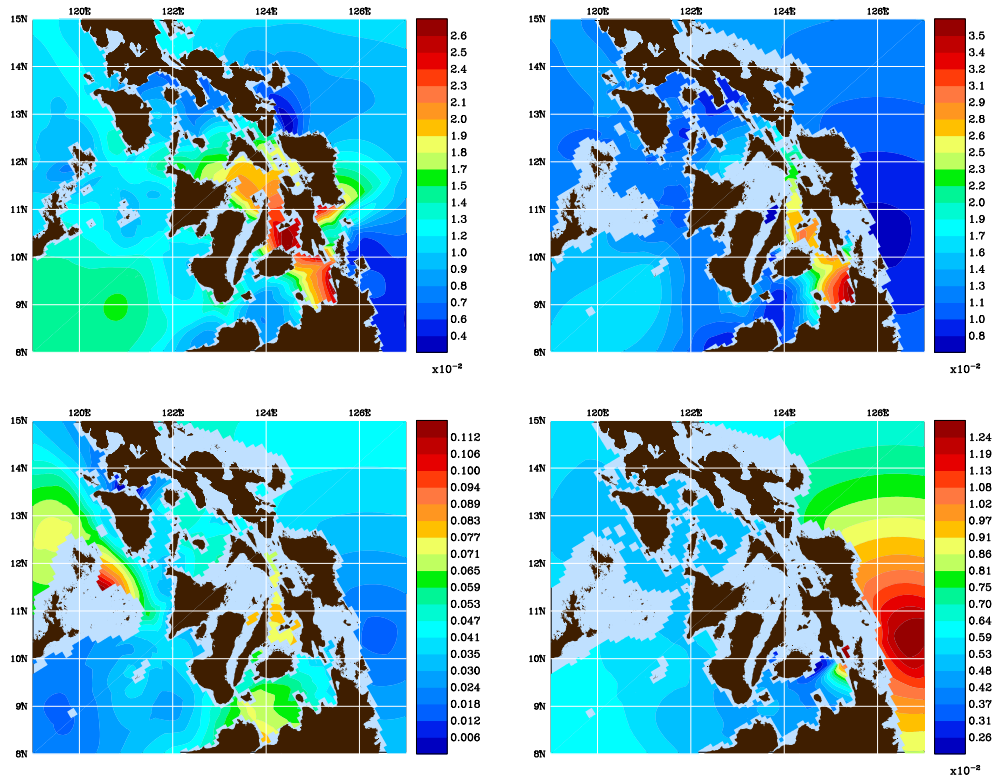


Figure 14: Chlorophyll ( $\mu\text{mol/Kg}$ ) OA Fields using the FMM at Level: (Top - Left) 0m; (Top - Right) 10m; (Bottom - Left) 50m; (Bottom - Right) 160m.

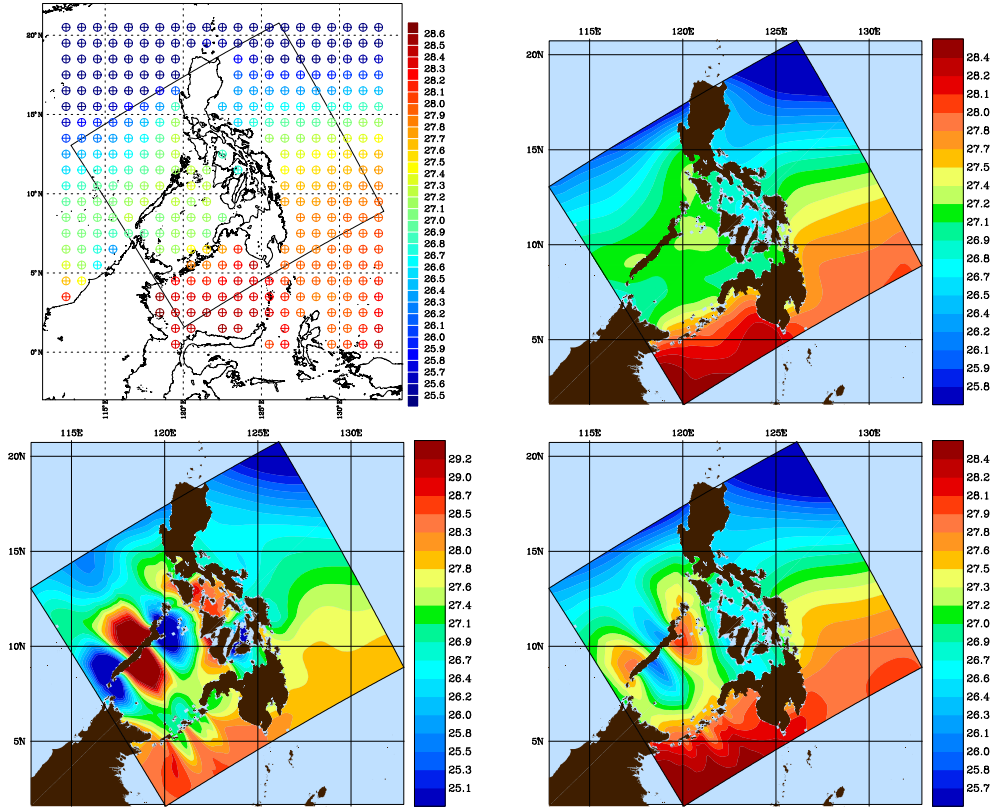


Figure 15: (Top - Left) World Ocean Atlas 2005 (Spliced February and Winter Climatology) in situ temperature ( $^{\circ}\text{C}$ ) at 0.0m; Temperature ( $^{\circ}\text{C}$ ) OA Fields using the Fast Marching Method at the surface (0m) using the following scheme and scales: (Top - Right) First order FMM and  $L_0 = 540\text{km}$ ,  $L_e = 180\text{km}$ ; (Bottom - Left) First order FMM and  $L_0 = 1080\text{km}$ ,  $L_e = 360\text{km}$ ; (Bottom - Right) Higher order FMM and  $L_0 = 1080\text{km}$ ,  $L_e = 360\text{km}$ .

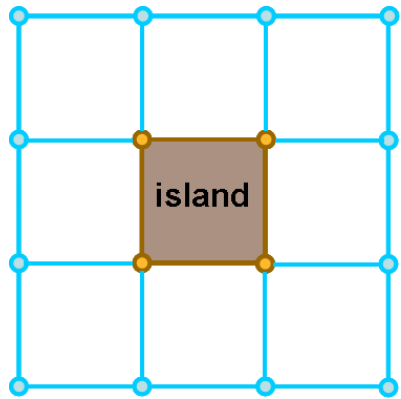


Figure 16: Example of an idealized (multiply-connected) domain having an island.

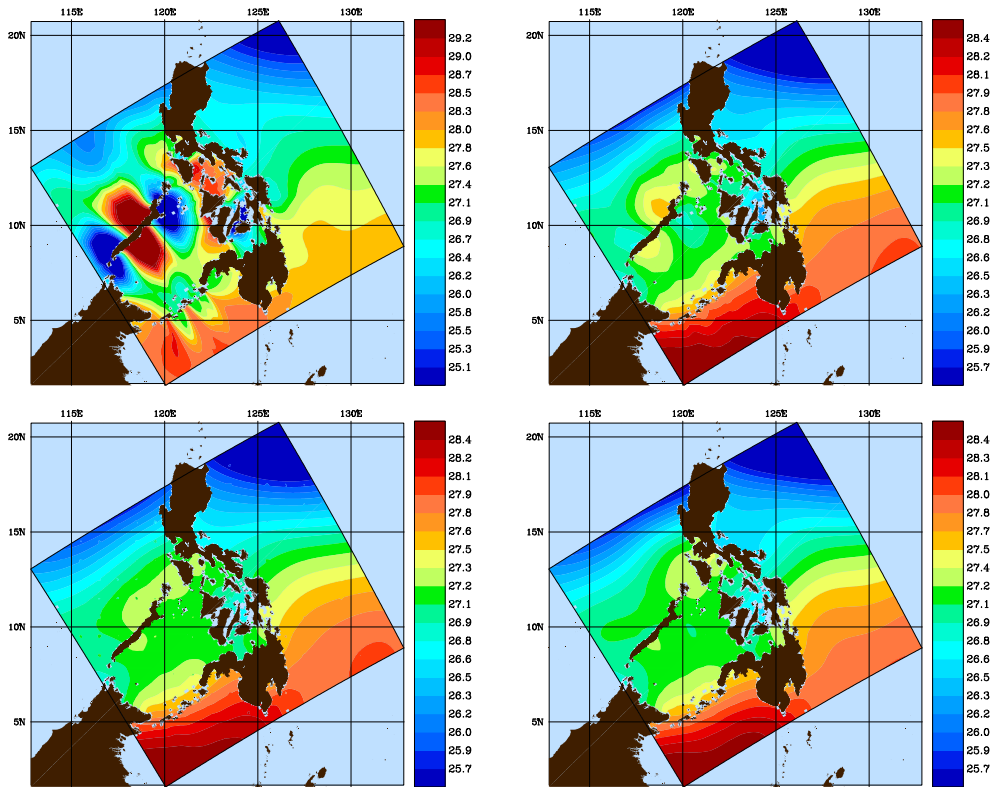


Figure 17: Temperature ( $^{\circ}\text{C}$ ) OA Fields at the surface (0m) (scales  $L_0 = 1080\text{km}$ ,  $L_e = 360\text{km}$ ) using the: (Top - Left) FMM; (Top - Right) FMM and removal of problematic data; (Bottom - Left) FMM and introducing process noise; (Bottom - Right) FMM and applying dominant singular value decomposition (SVD) of a-priori covariance.